R-746

SIRU DEVELOPMENT - FINAL REPORT
VOLUME II
GYRO MODULE

by

Roscoe Cooper
Thomas Shuck

June 1973

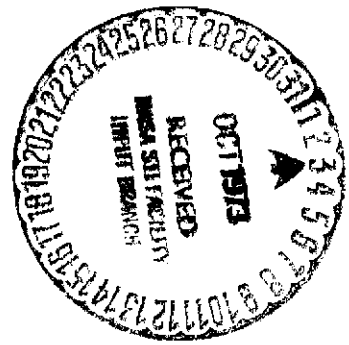

CHARLES STARK DRAPER LABORATORY

MASSACHUSETTS INSTITUTE OF TECHNOLOGY

CAMBRIDGE, MASSACHUSETTS, 02139

R-746

SIRU DEVELOPMENT - FINAL REPORT
VOLUME II
GYRO MODULE

by

Roscoe Cooper
Thomas Shuck

June 1973

CHARLES STARK DRAPER LABORATORY
MASSACHUSETTS INSTITUTE OF TECHNOLOGY
CAMBRIDGE, MASSACHUSETTS

Approved: _____ Date: May 31, 1973
J. P. GILMORE

Approved: _____ Date: June 8, 1973
N. E. SEARS

Approved: _____ Date: 6 Jun 73
D. G. HOAG

ACKNOWLEDGEMENT

This report was prepared under our Project No. 55-32600, sponsored by the Lyndon B. Johnson Space Center of the National Aeronautics and Space Administration through Contract No. NAS9-8242.

The successful development of the SIRU system to its present state of hardware, software and analytical maturity results from the dedicated efforts of many people from the NASA L. B. Johnson Space Center and the C. S. Draper Laboratory.

The technical and historical material presented in this volume of the SIRU Development Final Report was to a large extent contributed by the people who performed the original design and evaluation tasks. The major contribution by the authors has been in the collection, composition, direction and editing control of assembled material.

Special mention is due to the following for major contributions pertaining to their area of interest

Julius Feldman
Siegbert Katz
David Swanson

and to Jerold Gilmore and Robert Booth whose knowledge and assistance in the preparation of this report have been invaluable.

The work performed by Stephen Helfant with Linda Willy and Angela Desmond in editing and preparing the document for publication deserves special recognition. To the Apollo Publications Group with special mention to Ellen Hurley goes our sincere appreciation.

The publication of this report does not constitute approval by the National Aeronautics and Space Administration of the findings or the conclusions contained therein. It is published only for the exchange and stimulation of ideas.

R-746

SIRU DEVELOPMENT FINAL REPORT

ABSTRACT

This report presents a complete description of the development and initial evaluation of the Strapdown Inertial Reference Unit (SIRU) system sponsored by the NASA Johnson Space Center under Contract NAS9-8242.

The SIRU configuration is a modular inertial subsystem with hardware and software features that achieve fault tolerant operational capabilities. The SIRU redundant hardware design is formulated about a six gyro and six accelerometer instrument module package. The modules are mounted in this package so that their measurement input axes form a unique symmetrical pattern that corresponds to the array of perpendiculars to the faces of a regular dodecahedron. This six axes array provides redundant independent sensing and the symmetry enables the formulation of an optimal software redundant data processing structure with self-contained fault detection and isolation (FDI) capabilities.

This report consists of four volumes.

Volume I, System Development, documents the system mechanization with the analytic formulation of the FDI and processing structure; the hardware redundancy design and the individual modularity features; the computational structure and facilities; and the initial subsystem evaluation results.

Volume II, Gyro Module, is devoted specifically to the Gyro Module, the inertial instrument and its digital strapdown torque-to-balance loop, the mechanical, thermal, and electronic design and function, test procedures and test equipment and performance results and analysis.

Volume III, Software, documents the basic SIRU software coding system used in the DDP-516 computer. The documentation covers the instrument compensation software, reorganizational and FDI processing, and the inertial attitude and velocity algorithm routines as well as servicing, input/output, etc. software.

Volume IV, Accelerometer Module, is devoted specifically to the Accelerometer Module, the inertial instrument and its digital strapdown torque-to-balance loop, the mechanical, thermal and electronic design and function and performance results and analysis, as it differs from the Gyro Module.

In addition to this report, SIRU Utilization Report R-747, has been issued documenting analyses, software and evaluation activities in the application of advanced statistical FDI algorithms, calibration and alignment techniques to the SIRU system.

April 1973

TABLE OF CONTENTS

PRECEDING PAGE BLANK NOT FILMED

LIST OF ILLUSTRATIONS

LIST OF ILLUSTRATIONS (CONT)

DICTIONARY OF TERMS

AC	Alternating Current
AD	Acceleration-Dependent
A/D	Analogue to Digital
ADIA	Acceleration-Dependent Gyro Drift Due to Acceleration Along the Input Axis
ADOA	Acceleration-Dependent Gyro Drift Due to Acceleration Along the Output Axis
ADSRA	Acceleration-Dependent Gyro Drift Due to Acceleration Along the Spin Reference Axis
BD	Bias Drift
BeO	Beryllium Oxide
CSDL	Charles Stark Draper Laboratory
DC	Direct Current
EA	Electronics Assembly
GNC	Guidance, Navigation and Control
GSE	Ground Support Equipment
H	Angular Momentum about the Spin Axis
IA	Input Axis
IC	Inertial Components
ID	Independent Drift
INT	Interrogate Pulse
IRIG	Inertial Reference Integrating Gyro
K	Compliance
+LDFF	Positive Level Detect Flip-Flop
MIT	Massachusetts Institute of Technology
MTBF	Mean-Time-Between Failures
NASA	National Aeronautics and Space Administration
NBD	Normal Bias Drift
OA	Output Axis
PIP	Pulsed Integrating Pendulum
PIPA	Pulsed Integrating Pendulous Accelerometer
PIRIG	Pulsed Inertial Reference Integrating Gyro

PMT	Permanent Magnet Torquer
PPM	Part Per Million
PPS	Pulses Per Second
PTE	Pulse Torque Electronics
PTTB	Pulse Torque-To-Balance
PVR	Precision Voltage Reference
RIP	Redundant Instrument Package
SA	Spin Axis
SDF	Single Degree-Of-Freedom
SF	Scale Factor
SG	Signal Generator
SIRU	Strapdown Inertial Reference Unit
SRA	Spin Reference Axis
TG	Torque Generator
TMSFF	Torque Motor Set Flip-Flop
TP	Test Point
TSRFF	Torque Switch Reset Flip-Flop
W_{IA}	Angular Rate About The Input Axis

1.0 Introduction

Volume II of the SIRU Development Final Report describes the design and performance features of the gyro module. Volume I provides an overview of all aspects of the SIRU Development program including mechanization, hardware, software, reliability assessment and performance. Volume III consists of a detailed description of the system software including assembly listings and load maps.

1.1 System Description

A brief description of the SIRU system is provided here as an aid in associating the function of the gyro module with the other system elements.

The redundant Strapdown Inertial Reference Unit (SIRU) contains design features developed to provide an optimum combination of reliability and maintainability in a desirable size and weight configuration. Reliability results from the geometric redundancy afforded by a unique arrangement of six gyroscope and accelerometer pairs. Each pair is oriented such that their input axes (IAs) correspond to the array of normals to the faces of a dodecahedron, lie in the orthogonal planes of the structure referenced triad, and are displaced from the triad axes by a unique spherical angle (approximately 31.7^{o}).

This symmetry yields optimal redundant reorganization data processing with a minimal error propagation (Table 1.1). Software routines, by means of instrument output comparisons, permit failure isolation for up to two of the six instruments of each type, detection for a third failure and continued satisfactory operation after the failure of three gyroscopes and three accelerometers. The reliability resulting from this design feature is compared to other redundant arrangements in Fig. 1.1. Maintainability results from the fault isolation capability and the replaceable, modularized, packaging arrangement made possible by the strapdown configuration. The Redundant Instrument Package (RIP) consists of a mounting and alignment structure to which the six gyroscope and six accelerometer modules are mounted. The assembled RIP is shown in Fig. 1.2. Each instrument module consists of a prealigned gyroscope or accelerometer packaged with its normalizing and calibrating electronics as an interchangeable sealed unit. Access to each module for inspection, servicing or replacement is available at the front of the RIP. Size and weight characteristics, even in this development model compare favorably with alternate redundant systems. The RIP occupies a volume of approximately one cubic foot, weighs 63 pounds and requires 183 watts of power.

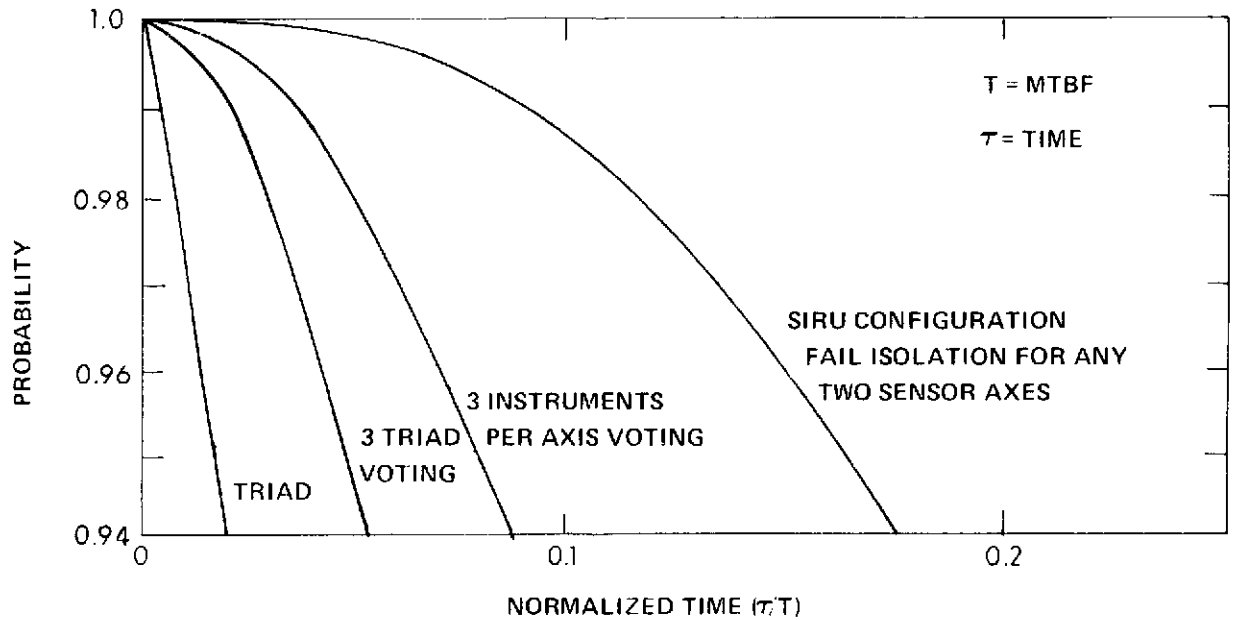

Fig. 1.1 Mission Success Probability

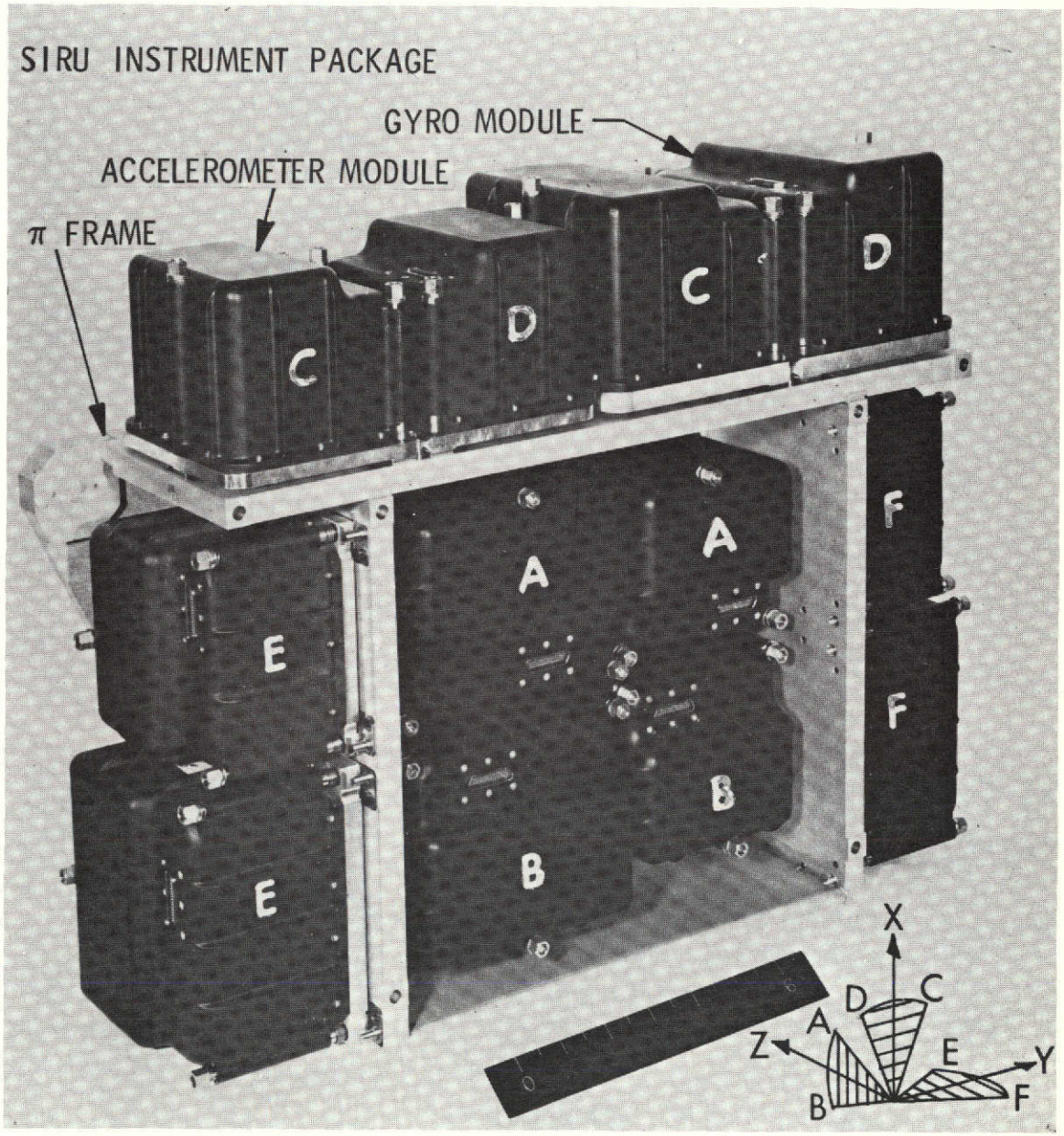

Fig. 1.2 SIRU Redundant Instrument Package

Table 1.1

SIRU Performance With Instrument Failures
Versus
An Operational Triad System

Instrument Failures	Standard Deviation (Worst-Case Axis Solution)	Ratio of Deviation (SIRU Solution to a 3-axis System)
None	0.707σ	0.707
1 (6 Combinations)	0.927σ	0.816
2 (15 Combinations)	1.349σ	1.000
3 A (10 Combinations)	1.349σ	1.176
3 B (10 Combinations)	2.890σ	1.902

1.2 Gyro Module

Contained in the gyro module are the inertial sensor and the electronics which generate a signal quantized in incremental input angle. The module requires basic supply voltages and timing pulses from the electronic assembly. The module is mechanically aligned to its mounting pads, temperature controlled and normalized so that each module presents, within the tolerances specified, an identical interface with the SIRU system.

This volume presents a detailed description of the design, operation, performance and test of the gyro module and its circuit components. The presentation is divided into four principal sections as follows:

1. Technical Description—Provides a detailed description of the operation of the gyro module and each of its component elements.
2. Gyroscope Instrument Status—Provides a review of the design, production, reliability and life of the gyros used in the SIRU program.
3. Gyro Module Performance—Presents gyro and module drift, scale factor and alignment summaries.
4. Gyro Test—Describes the test equipment and the test routines performed on each module.

2.0 Gyro Module—Technical Description

The function of the gyro module is to sense the component of rotation being applied along its IA and deliver as its output a sequence of weighted pulses which defines the magnitude and sign of the rotation. The action is accomplished by closing a ternary loop around the gyro by means of precision current pulses to the gyro torquer. The general specification requirements for the gyro module including scale factor and drift parameters, input and output power and signal characteristics and tolerances, thermal limitations and connector pin designations are provided in Appendix A.

Modularized inertial component (IC) assemblies were incorporated in the SIRU system to meet the requirement for in-flight maintenance. The modules are configured mechanically, thermally, and electrically to make replacement as simple and straightforward as possible. To accomplish a removal it is only necessary to loosen three screws conveniently located on the module, disengage a single multi-pole connector and lift the module from the π-frame. Replacement reverses the procedure. This capability for simple in-flight replacement depends on the prealigned, normalized condition of each module, the accuracy of the remount alignment provision, the rugged construction of the assembly, the accuracy and stability of the prealignment operation and the self-calibration features of the SIRU software.

The functional block diagram of the gyro module is shown in Fig. 2.1. A family tree diagram identifying drawings and specifications covering the major subassemblies is provided in Table 2.1. The gyro module consists of the following components:

1. Gyro - 18 IRIG Mod B
2. Gyro Pulse Torque Electronics
3. Interpolator/Compensator
4. 8 Volt Power Supply
5. Torquer Tuning Network
6. Bandpass Preamplifier
7. Temperature Controller
8. Normalization Assembly

The location of these components in the gyro module is shown in Fig. 2.2.

The following description of the function and principle features of each component is essentially identical to that provided in Volume I, Chapter 3 except that additional circuit information for the temperature controller is included here.

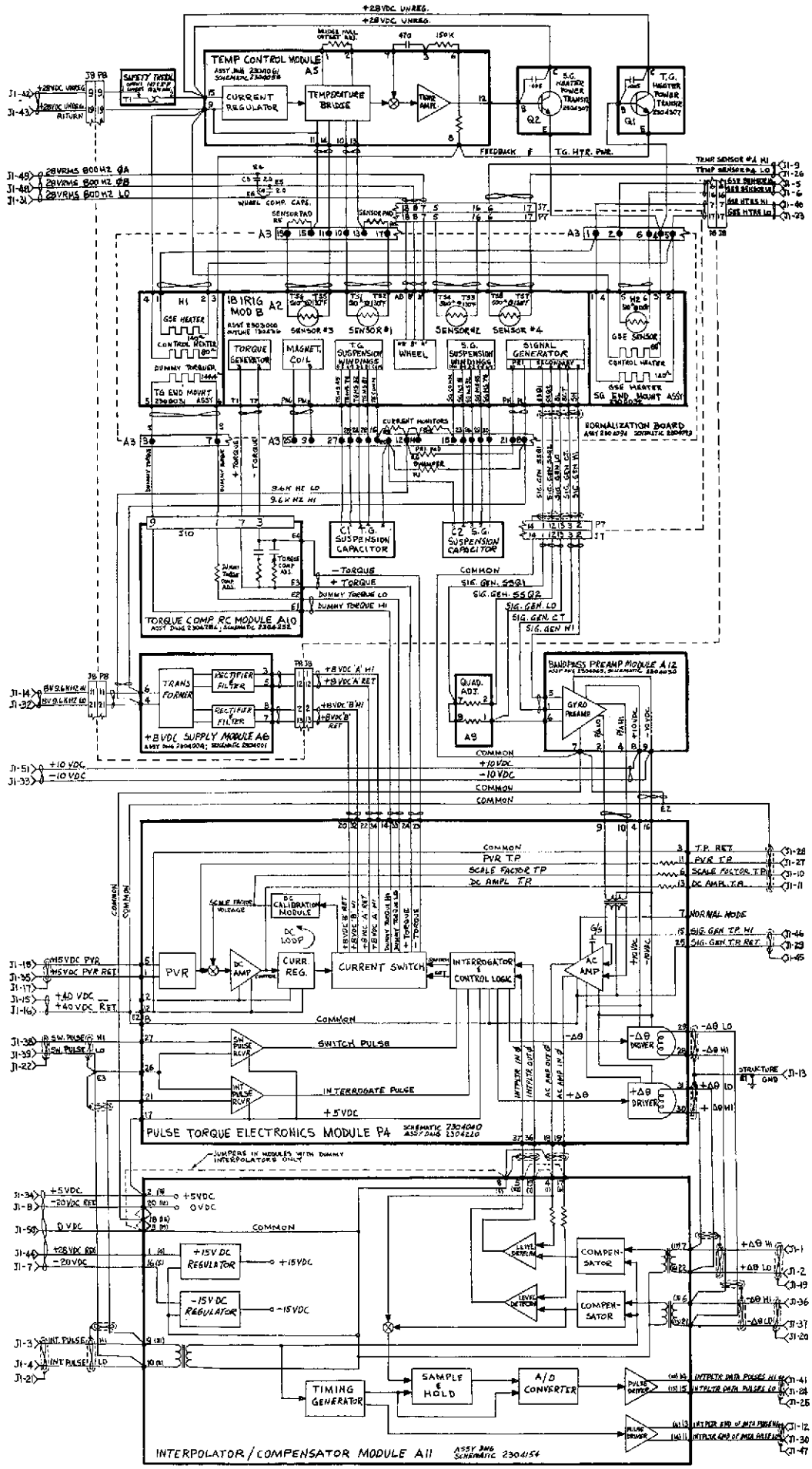

SIRU GYRO MODULE - TWO WIRE MECH DWG.

REF SIRU GYRO MODULE WIRING LIST REV 12

B. KATZ
2-26-70

Table 2.1

Gyro Module Family Tree

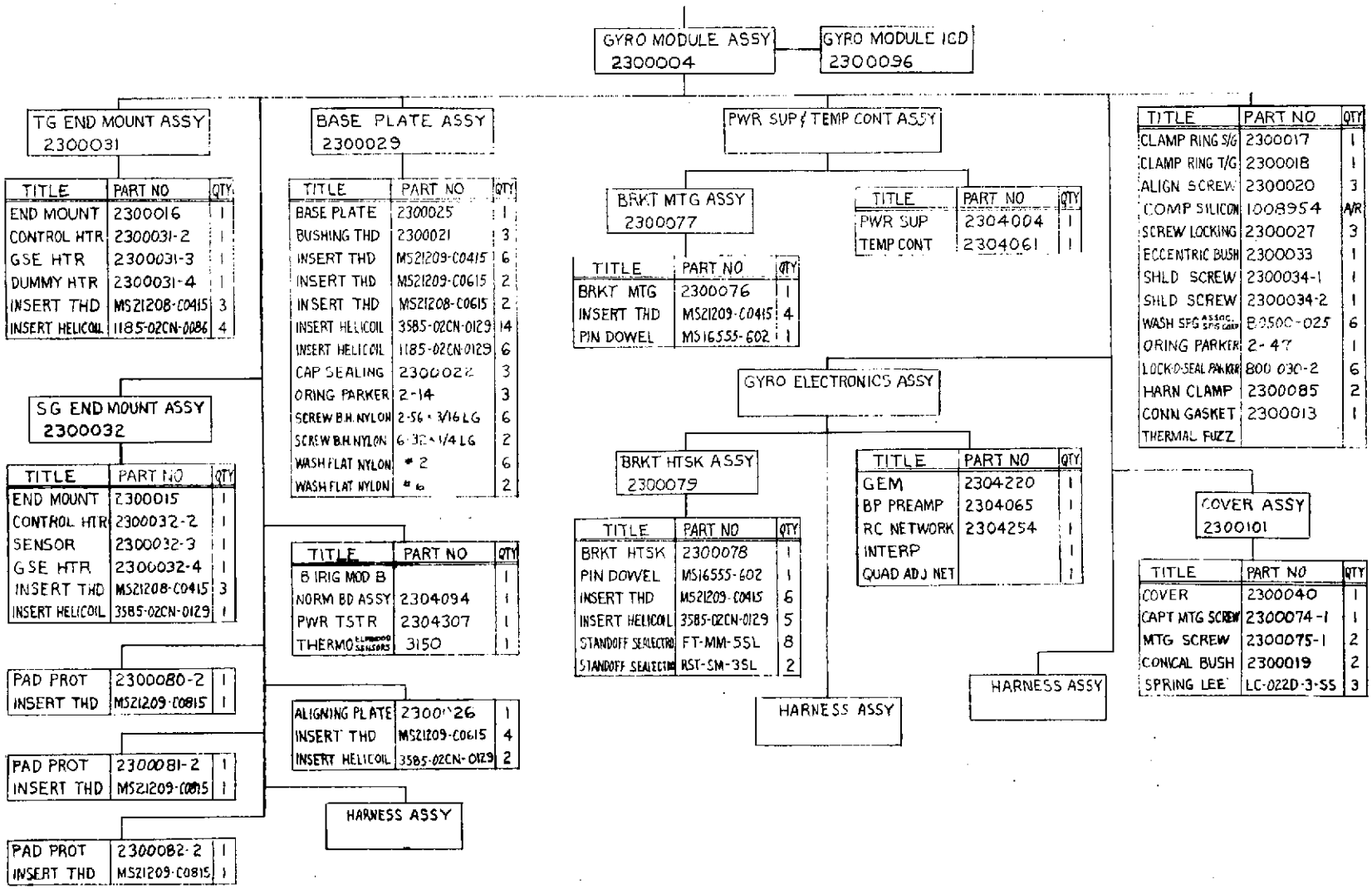

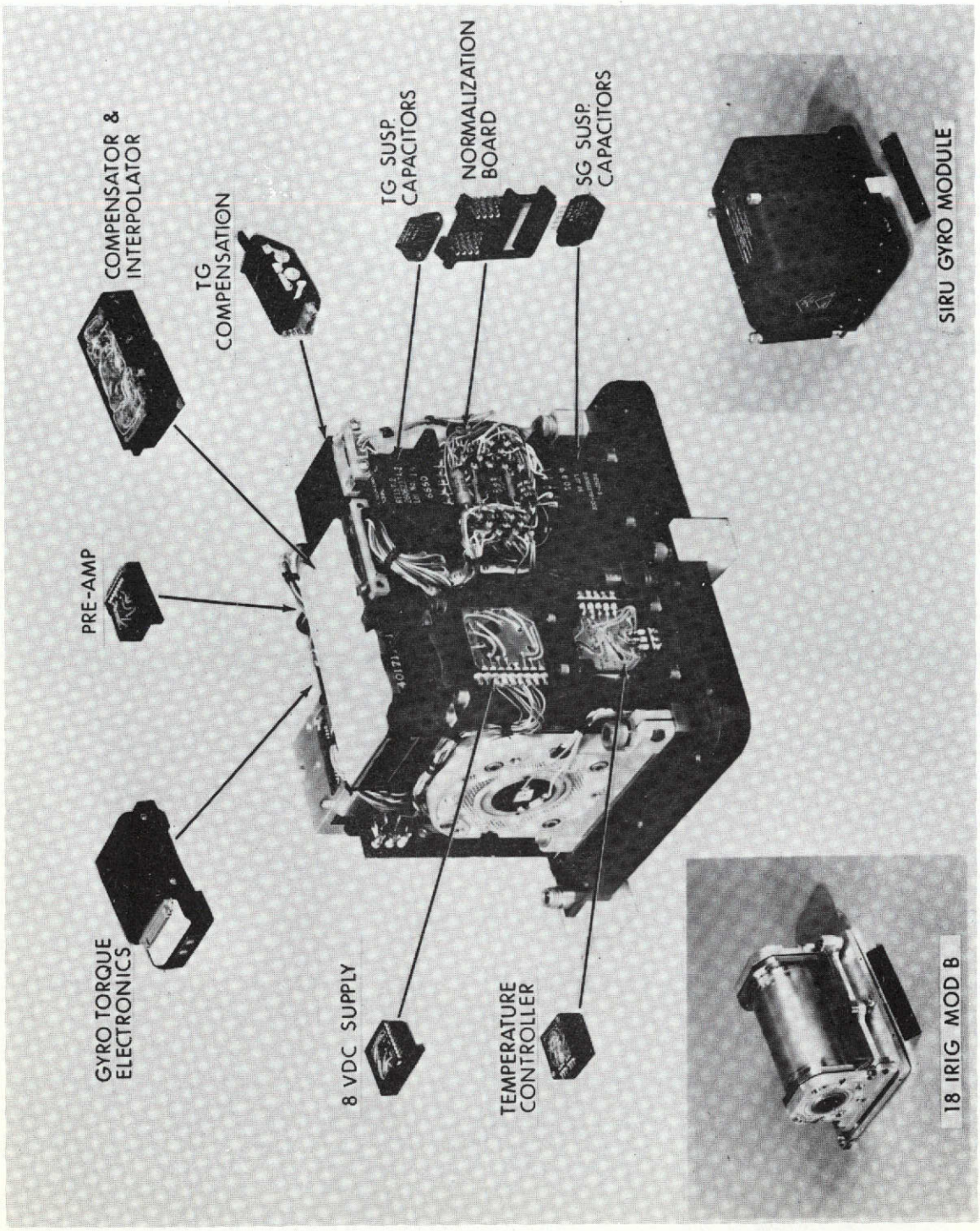

Fig. 2.2 Gyro Module Subassemblies

1. Gyro - 18 IRIG Mod B

General Description

The 18 IRIG is an advanced design, gas bearing instrument specifically designed by the Draper Laboratory for the strapdown application. Figure 2.3 is a cutaway view of the 18 IRIG Mod B 420 series gyroscope showing the various components. The wheel, made from a fine-grained, hot pressed, alumina ceramic, rotates at 24,000 rpm on a spool type gas bearing generating an angular momentum of 150,000 gm-cm^2/sec. The ceramic encapsulated motor stator enhances float mass stability, and reduces the possibility of condensed contaminates on the bearing surfaces.

The float, which houses the wheel and stator, is fabricated from a high-precision elastic-limit beryllium which combines low density with excellent stability. It is surrounded by and floated in a high density, controlled viscosity, chemically inert dielectric fluid maintained at a precisely controlled temperature. The fluid thus isolates the float from environmental inputs and provides the damping which is an essential characteristic of the single degree of freedom (SDF) integrating gyroscope. The float inertias and compliances about the spin axis (SA) are matched to those of the IA to minimize dynamic errors from these sources.

The permanent magnet torquer (PMT) is capable of developing 150,000 dyne-cm of torque, sufficient to balance an input rate of one rad/sec. Tapered electromagnetic suspensions provide radial and axial stiffness capable of restraining the float at the rated input angular velocity. The angular position of the float from its null location is measured by a multiple E type signal generator (SG). SG sensitivity when excited by an 8v, 9600 Hz source is 20 mv/milliradian.

The instrument is hermetically sealed within a Mumetal shroud to augment magnetic isolation, aid heat transfer control and protect the gyro from unauthorized adjustment. Temperature control and monitoring are provided by four nickel wire wound sensors controlling heaters which are located on the gyro end mounts. The complete instrument measures approximately 2 inches in diameter and 3 7/8 inches long. Weight is 1.15 pounds. A summary of the average value and standard deviation for characteristics of the 18 IRIG Mod B 420 series gyro population is presented in Table 2.2.A.

The gyro in the SIRU system is operated in a closed loop where the torques on the float are restrained by torques developed by the torque generator (TG). See Fig. 2.4. An angular rate imposed about the IA of the gyro produces a torque about

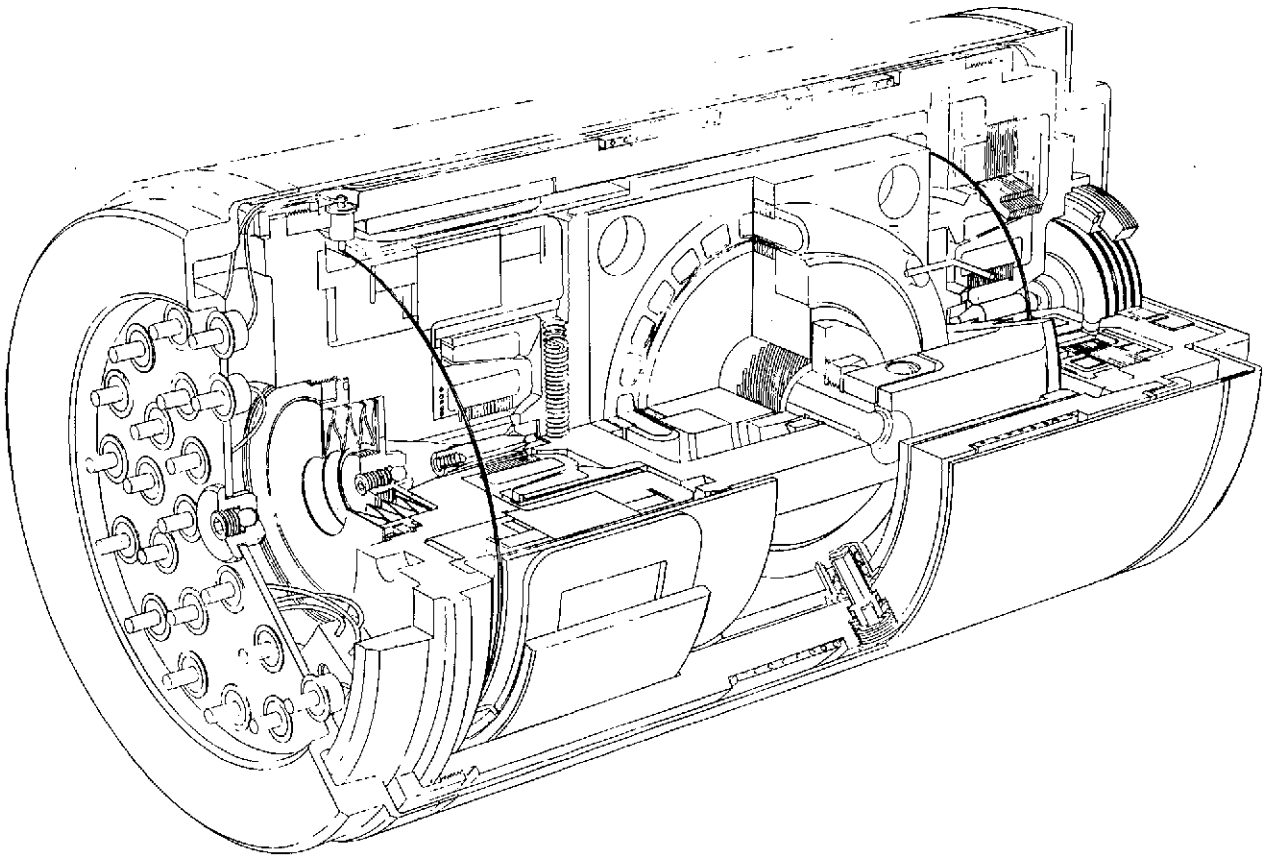

Fig. 2.3 18 IRIG Mod B Cutaway

Table 2.2.A

] 18 IRIG Mod B – 420 Series Population Characteristics

			$\bar{x}$	σ
Output Axis Damping	dyne-cm-sec		7.16×10^5	4.2×10^4
Angular Momentum	dyne-cm-sec		1.51273×10^5	1.12×10^3
Output Axis Inertia	gram-cm^2		226.24	0.36
Inertia Mismatch (I_{SA}-I_{IA})	gram-cm^2		14.5	1.0
Transfer Function	mv/mrad		4.38	0.22
Wheel Runup Time	seconds		9.2	0.34
Wheel Rundown Time	seconds		51.7	3.3
Wheel Power	Watts		5.15	0.2
Wheel Breakaway Voltage	volts	SA	14.8	1.4
		SA	18	2.4
		SA	18.8	2.8
Torque Command Sensitivity (S_{tg}/ H)	mrad/sec/ma		7.0 to (settable)	7.8
Variations With:				
Temperature	ppm/°F		2.4	5.3
Float Radial Position	ppm/0.0001"		6.6	5.8
Float Axial Position	ppm/0.0001"		1.8	6.3
Float Angle	ppm/mrad		45.4	5.5
ΔS_{tg}/ H (+to - Current at 60 ma DC)	ppm		9.2	73

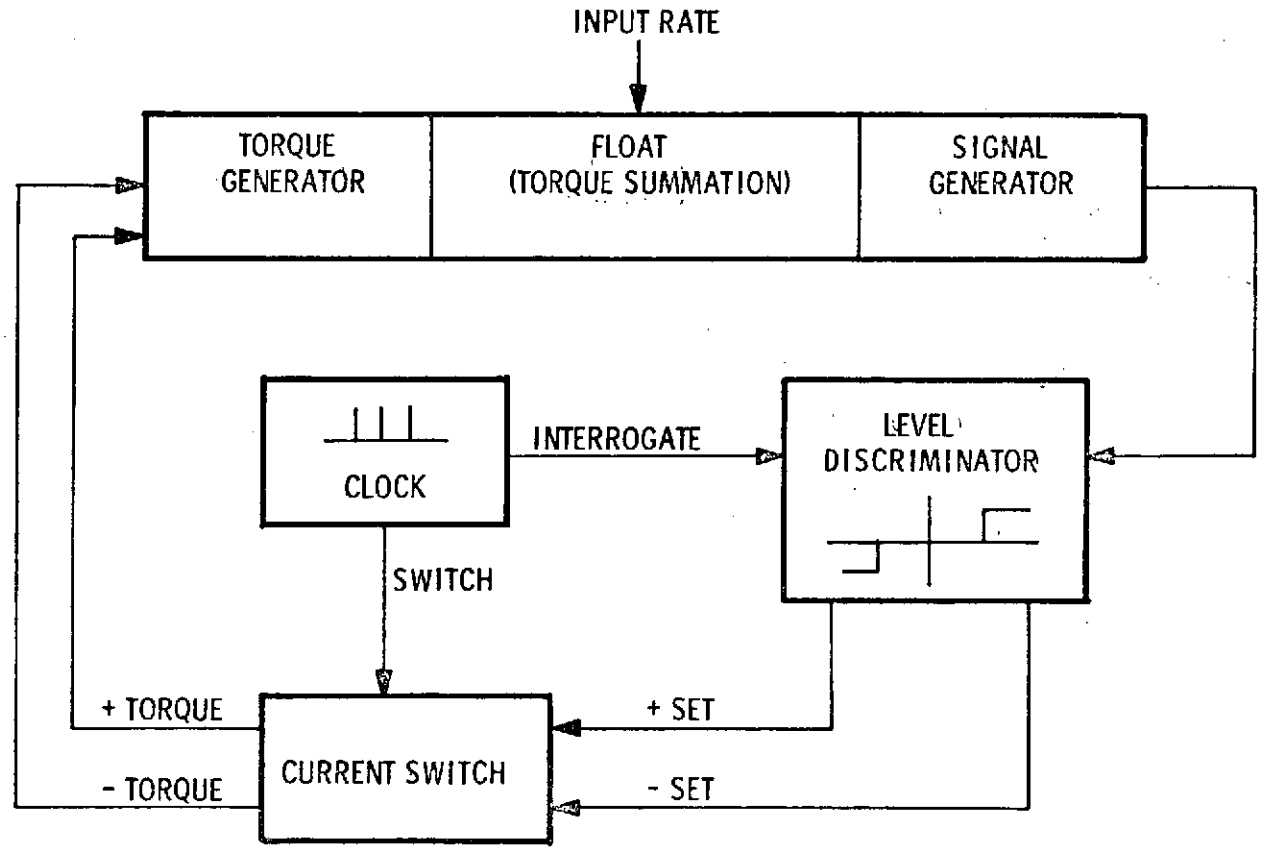

Fig. 2.4 Block Diagram-18 IRIG Closed Loop

its output axis (OA) and causes the float to rotate from a signal null position. The direction and magnitude of the float rotation are detected by the SG. When the SG output voltage reaches a given threshold level, a discriminator provides a positive or negative set signal, depending on the polarity of the SG output voltage. These set signals are interrogated at a given frequency to switch a current pulse of fixed amplitude and duration to the TG winding. In the control loop mechanization, a principle error source is inaccuracy in the torque pulse area. For example, a torque pulse of 100 ma amplitude and 200 microseconds width exhibiting a variation from nominal of 10^{-4} ma in amplitude or 2×10^{-10} sec in width will cause an error in scale factor (SF) of one ppm.

Performance characteristics determined from acceptance test data for the 18 IRIG Mod B 420 series population are shown in Table 2.2.B. Average values and distribution of the population are shown.

2. Gyro Pulse Torque Electronics (PTE)

The output of the gyro PTE is incremental IA angle. The PTE receives the input from the gyro SG, evaluates the threshold level in the torque control logic, and, if ordered, supplies current pulses to the gyro TG as required to reduce the SG signal below the threshold. The width of the current pulse is controlled by timing pulses transmitted by the torque control logic and the amplitude of the current pulse is maintained by a feedback loop involving the comparison of a precision voltage reference (PVR) and a current sampling resistor. The current pulse is transmitted to the gyro TG through a current switch which is set by the torque control logic to provide the appropriate polarity. The operation of the PTE is described in detail below.

The output signal from the gyroscope is first amplified by a bandpass preamplifier, fed into the ac amplifier (x10) in the PTE and then to a comparator or threshold device.

As shown in the timing diagrams, Figs. 2.5 and 2.6, and the logic diagrams, Figs. 2.7 and 2.8, the comparator is strobed by the leading edge of the 4800 pps interrogate pulse (INT) which coincides with the peak of the 9600 Hz signal at the comparator. A phase adjustment tailored to each gyro is made to the SG signal in the bandpass amplifier to insure this relationship. If, at the instant of strobe (INT), the peak level of the amplified SG voltage exceeds the positive threshold level (equivalent to 44 $\widehat{\text{sec}}$ of gyro IA angle) and is in phase with the INT pulse, a positive level detect signal is generated which sets the positive level detect flip-flop (+LDFF)

Table 2.2.B

18 IRIG Mod B – 420 Series Population Characteristics

			$\bar{x}$	σ
AD Terminal Temperature Sensitivity	°/hr/g/°F	ADIA ADSRA	.020 .022	.075 .135
Initial Magnitude	°/hr/g	ADIA ADSRA	.675 -.750	1.530 1.185
9 Acceptance Tests A_1, A_2, A_3, Cooldown B_1, B_2, B_3, Cooldown C_1, C_2, C_3 Magnitude (Maximum Magnitude Across 9 Runs)				
BD	°/hr		-.437	.695
ADIA	°/hr/g		.053	.237
ADSRA	°/hr/g		-.011	.177
Stability (1σ Of Magnitude Across 9 Runs)				
BD	°/hr		.018	
ADIA	°/hr/g		.047	
ADSRA	°/hr/g		.024	
ADOA	°/hr/g		-.012	.024
ID	°/hr		-.285	.420
ΔK	°/hr/g^2		.291	.156
K_{10}	°/hr/g^2		-.011	.004

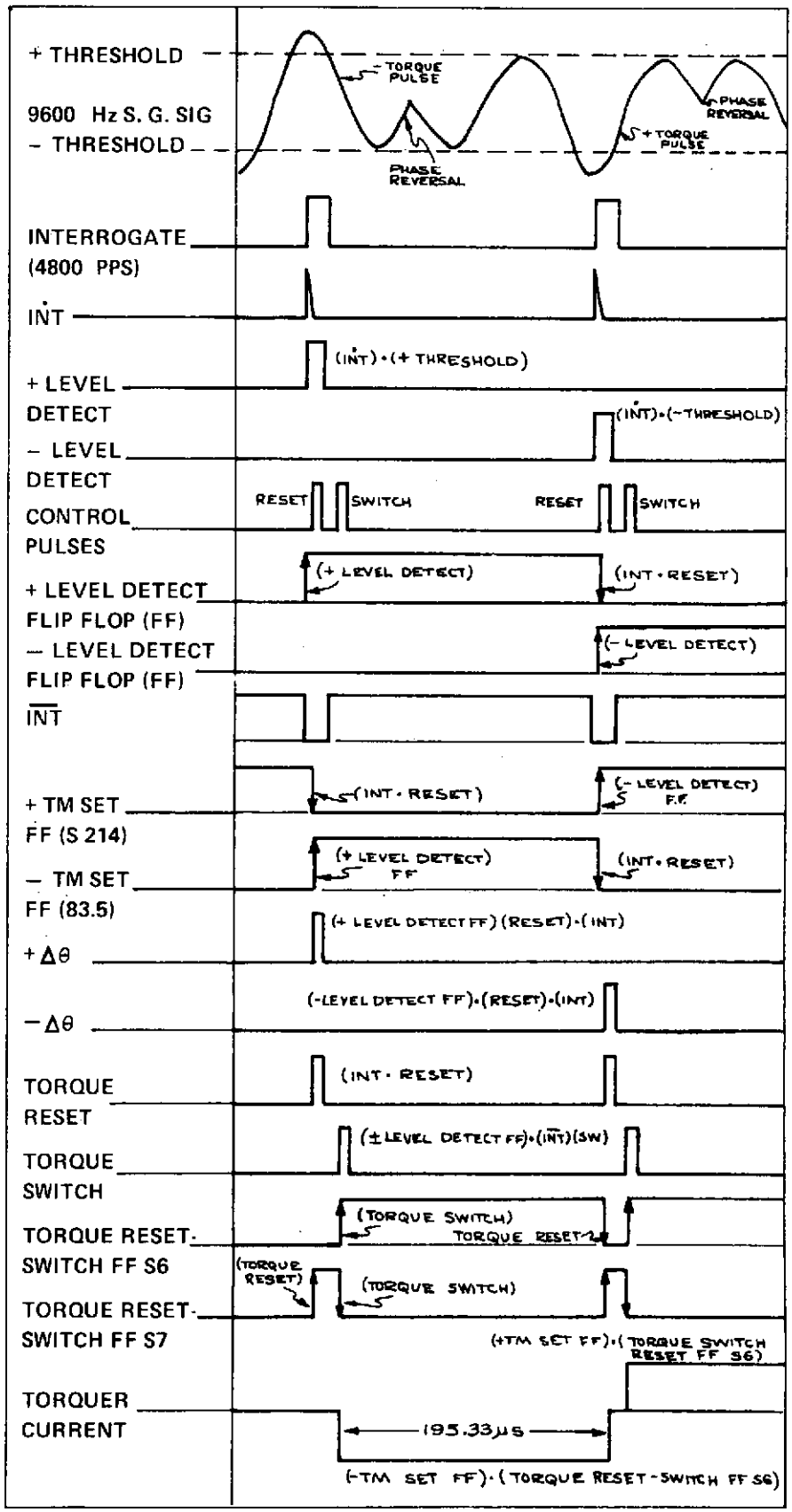

Fig. 2.5 PTE Timing Diagram

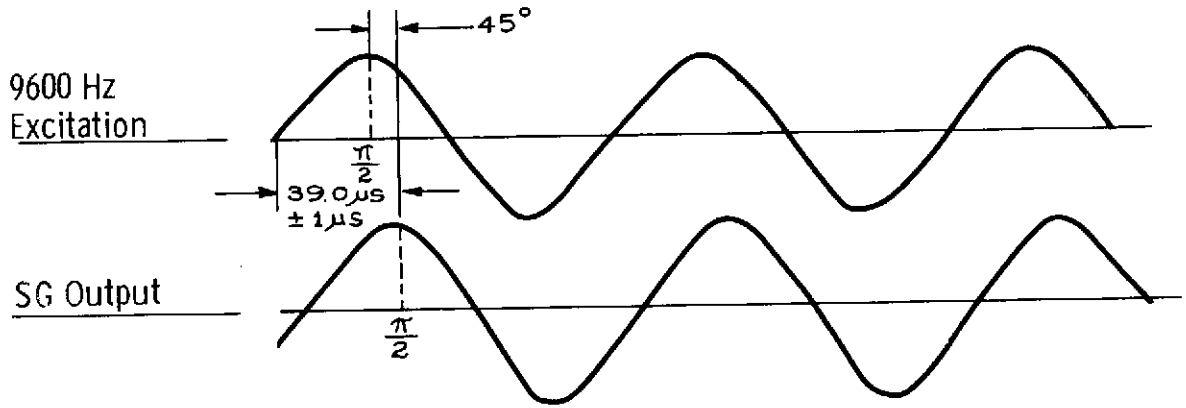

* 13.0208 μsec + 5 ppm absolute error

\+ Stability of set - reset pulse spacing 1 ppm over 24 hour period

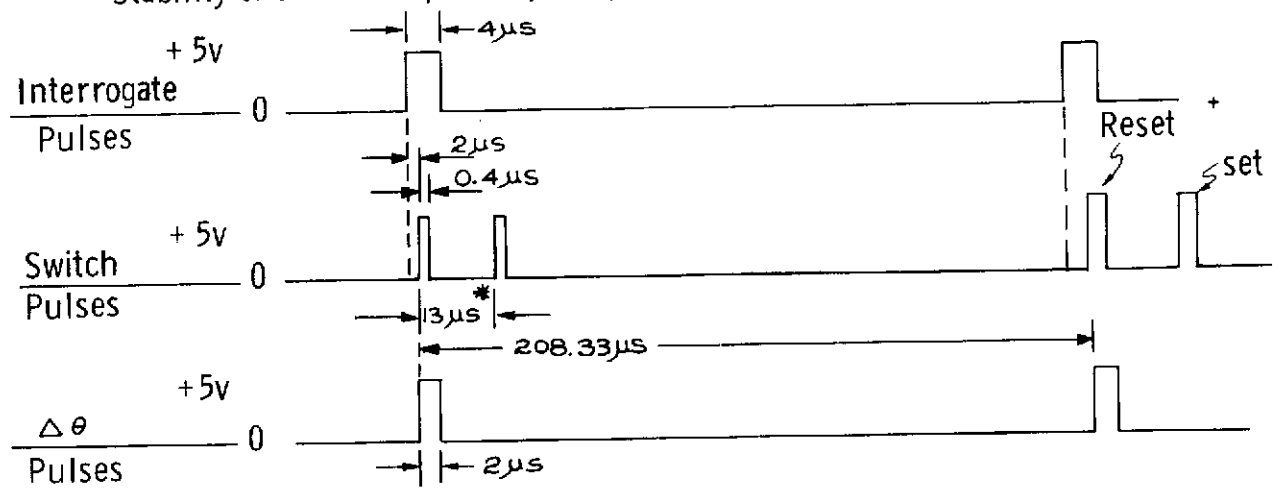

Fig. 2.6 SIRU Gyro Module - Timing

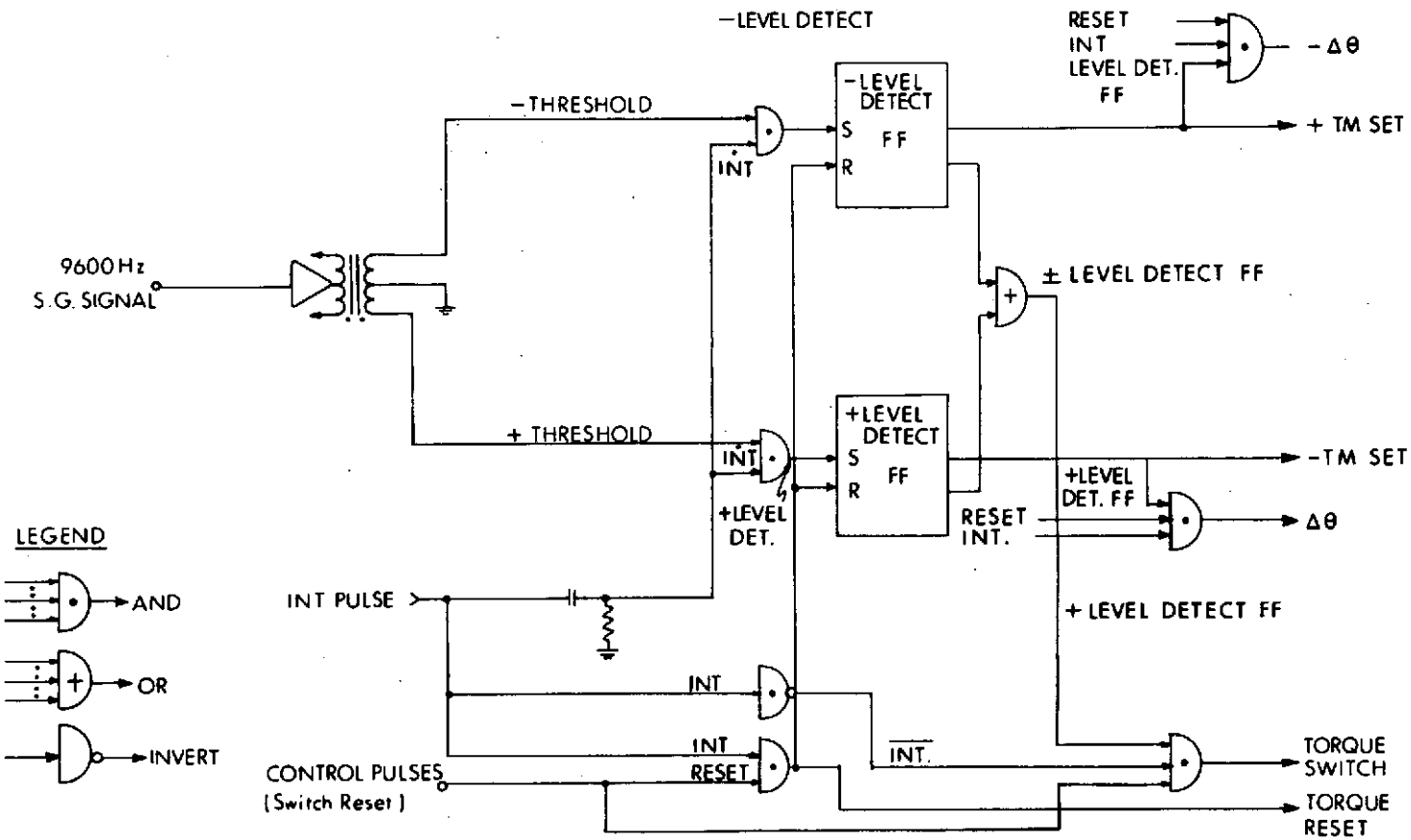

Fig. 2.7 PTE Logic

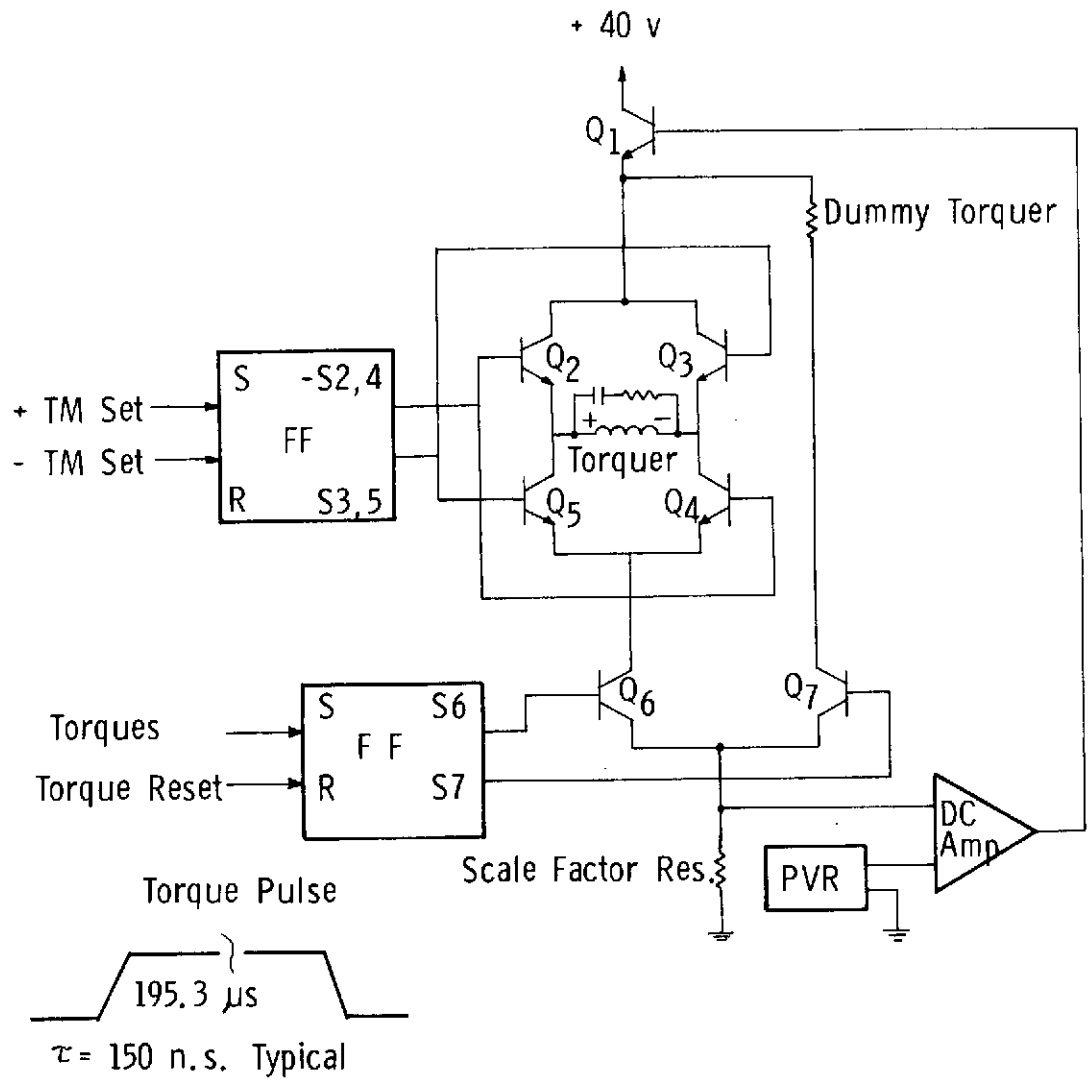

Fig. 2.8 PTE H Switch

to its positive state. The output of the +LDFF then sets the torque motor set flip-flop (TMSFF) to its negative state (S2, 4=-; S3, 5=+). The positive output of the TMSFF turns on Q3 and Q5 which sets up the current switch for a negative torque current command. The output of the +LDFF is also summed with the reset and INT pulses in the $+\Delta\theta$ AND gate to generate a $+\Delta\theta$ pulse upon receipt of the reset pulse. This $\Delta\theta$ pulse goes to the computer. The output of the +LDFF also goes to the torque switch AND gate where it is summed with the INTand the switch pulses. When the switch pulse occurs, a torque switch pulse is generated which sets the torque switch reset flip-flop (TSRFF) to its switch state (S6=+; S7=0). The output of the TSRFF turns on Q6 and turns off Q7 which sets up the current switch to send current to the torquer winding instead of the "dummy" torquer. The INT pulse (4 microseconds wide) starts 195.33 microseconds later, followed 2 microseconds later by the reset pulse (0.4 microseconds wide). These pulses are summed in the torque reset AND gate which sends a pulse to the TSRFF switching it back to its reset state (S7 = +; S6 = 0). The output of TSRFF turns on Q7 and turns off Q6 returning the output of the current switch to the "dummy" torquer. A similar sequence occurs when the negative threshold level is exceeded except that a positive torque current and a negative $\Delta\theta$ are generated.

The duration and amplitude of the torque current pulse determine the torque delivered to the gyro by each pulse and thus determines the quantization constant for the system (nominal is 44 $\widehat{\text{sec}}$). The duration is determined by the time between the set and reset pulses and is 195.33 microseconds. A stability of 1 ppm over a period of 24 hours is characteristic of the SIRU performance. The current amplitude is maintained stable by the torque current loop, Fig. 2.9. This control loop compares the voltage drop across a precision (secondary standard quality) resistor with a precision voltage reference (PVR). The difference voltage is amplified by the high gain dc amplifier and fed back to Q1 which controls the torque current voltage.

The stability and absolute magnitude of the torque current are, therefore, established by the PVR, the current sampling resistor (or SF resistor) and the high gain dc amplifier. For a given PVR and dc amplifier, the absolute magnitude of the current is determined by the SF resistor which is selected to match the measured gyro SF within 200 ppm. The SIRU loop has demonstrated a long term (one year) SF stability of 10 ppm.

Inputs to the torque control logic are by way of pulse receivers, one for the interrogate pulse train and one for the switch pulse train. The calibration stability of the module is largely dependent on the rise time characteristics of the pulse trains. Low noise performance is achieved using a single diode level "standoff"

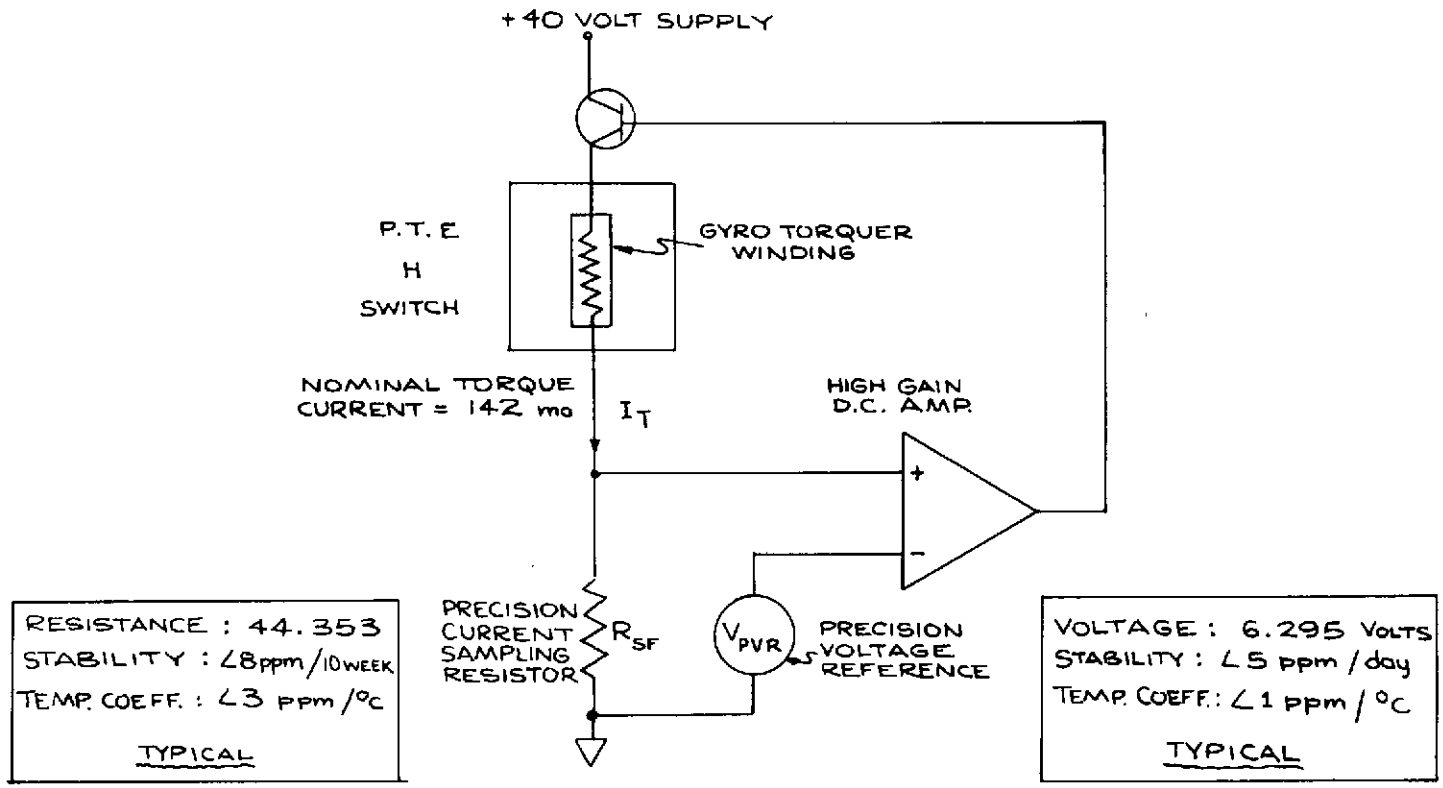

Fig. 2.9 Torque Current Loop

coupled to a fast rise, discrete, two stage pulse amplifier. Output $\Delta\theta$ lines are transmitted to the computer through line drivers to compensate for possible variation in transmission line length, performance characteristics and pickup. The line drivers consist of blocking oscillators designed to provide ground decoupling and a high level of cable drive power.

3. Interpolator/Compensator

The Interpolator/Compensator provides a dual function. As a compensator it substantially eliminates the effect of the dynamic characteristics of the gyro float and linearizes the gyro torque loop output response to the applied input rates. Without this compensation, lagging gyro float response to a torque pulse can result in multiple pulsing. In the uncompensated SIRU pulse torque-to-balance control loop at an interrogation rate of 4800 pps and with a time constant of 330 microseconds, obtained from the ratio of gyro float inertia to OA damping, multiple pulses occur. In the accelerometer loop with the 16 PIP Mod B, the accelerometer time constant is much smaller than for the gyro, and compensation for float dynamics is not required.

The float response to a single torque pulse provides insight into this effect of lagged response on closed loop operation. At the 4800 pps interrogation rate, (period = 207 microseconds) only 15% of the commanded travel has occurred by the time the next sample is made. Thus, at 4800 pps, an angular rate about the gyro input axis, W_{IA}, in excess of 15% of the full-on torque loop rate capability will result in at least one extra pulse. For example, consider an initial condition in which a steady state W_{IA}, is applied such that the float travel in a sampling period is slightly in excess of 15%. At sampling time (assume the float crossed over the torquing threshold exactly at a control loop sampling point) a restraining torque command pulse is issued. The float sums the steady state input and the pulse response. The input will exceed the pulse response over the next sampling interval leaving the float outside the threshold to trigger another torque pulse. The resulting output is two $\Delta\theta$ increments in response to an input slightly in excess of one $\Delta\theta$. For the next few sampling periods, the float response is dominated by the two successive torque pulses, resulting in a relatively long off time followed by another burst of two pulses. The indicated angle is averaged over the input interval, but the multiple pulsing has induced instantaneous errors. The resolution of the system is decreased from the resolution established by the $\Delta\theta$ value of each pulse. A compensation technique to eliminate this problem is shown in Fig. 2.10. Analog voltages, $\pm E$ compensated, are developed by generating a 206.3 microsecond pulse from a flip-flop circuit which is set and reset by the $\Delta\theta$ and interrogate pulses. This pulse, which is approximately the same length as the torque command (195.3 microseconds) is

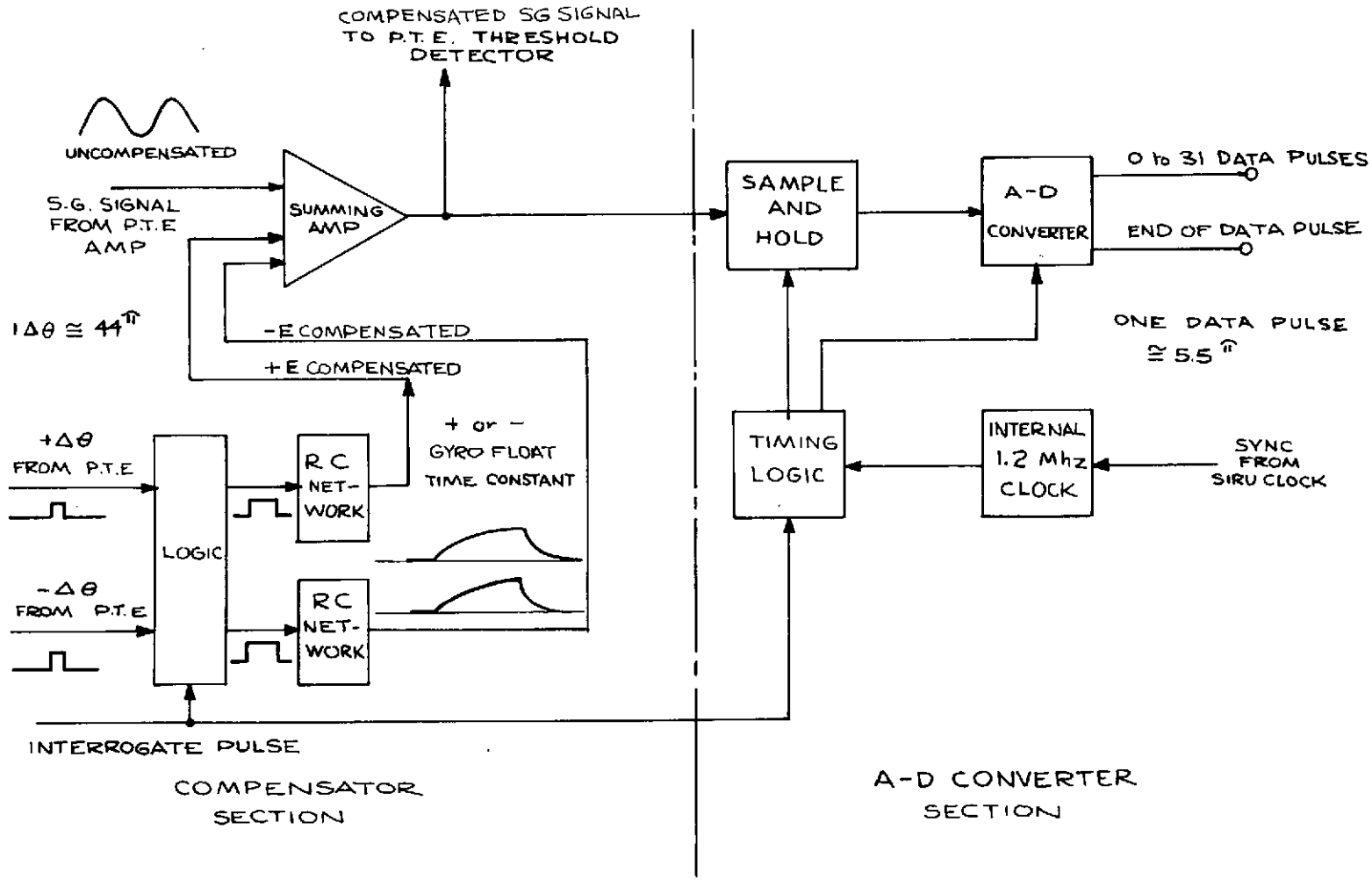

Fig. 2.10 Interpolator Block Diagram

integrated by an RC network to generate a voltage of the proper phase and magnitude. This voltage when summed with the gyro SG signal, compensates for the gyro float time constant and eliminates the multiple pulsing.

The effectiveness of this technique is illustrated in Table 2.3. This table presents the distribution of the pulse torque patterns for the compensated and uncompensated loop of a SIRU gyro module when operated at 1/4 of maximum rate (.25 rad/sec) and at an interrogation frequency of 4800 pps. The first column represents the number of times that a particular mode occurred; the second and third columns, the number of ON pulses and OFF pulses for that particular mode. The predominant 3 to 1 ratio of OFF to ON pulses indicates an input of 1/4 of maximum rate. The spread of pulse patterns from this 3 to 1 ratio is attributable to noise and variations in table rate. The uncompensated loop data characteristically has a burst of 3 ON pulses followed by 9 OFF pulses compared to 1 ON and 3 OFF for the compensated loop data.

Table 2.3
SIRU Gyro Module Moding Patterns at 4800 Hz

Number of Occurrances	Torquer On	Torquer Off
Without Compensation		
1678	2	6
205	2	7
382	3	8
4095	3	9
With Compensation		
1132	1	2
4095	1	3
1937	1	4

Input Rate: 0.25 radians/second

As an interpolator, once each interrogation period the unit samples and holds the analog compensated SG signal, performs an analog to digital (A/D) conversion, parallel shifts the digital data pulses into a serial register and finally sends the data accompanied by an end-of-data pulse to the computer. The data is quantized such that each data pulse is approximately 5.5 $\widehat{\text{sec}}$ or 1/8th of a 44 $\widehat{\text{sec}}$ $\Delta\theta$ pulse.

The timing of the data pulses and the end-of-data pulse are shown in Fig. 2.11.

4. 8 Volt Power Supply

The 8 volt power supply is a dual dc power supply with identical floated and isolated outputs. One +8v output supplies a zener regulator in the PTE which in turn provides excitation to the polarity determining logic of the H switch (See Fig. 2.8). The other +8v output also supplies a zener regulator for the torque-no torque (set-reset) logic of the H switch. In order to reduce capacitance to ground and thereby minimize switching transients, the input transformer is designed for minimum interwinding capacitance and the supply is located in the module with the PTE to reduce lead capacitance. The 8v, 9600 Hz excitation is used because it is available in the module, simplifying the module wiring interface, and isolation of the 8v supply is easier with ac. Because of inherently good regulation and the relatively high operating frequency, the size of the transformer and the filter components can be small. See schematic drawing number 2304009.

5. Torquer Tuning Network

This module contains two series RC networks which are connected in parallel with the gyro torque generator coil. See Fig. 2.12. The networks' function is to tune the coil so that minimum scale factor deviation with rate is achieved. The unit also contains a trim resistor which is in series with a "dummy" torquer. This trim resistor is used to adjust the "dummy" torquer resistance to the actual dc resistance of the torquer. The "dummy" torquer is a non-inductive heater whose resistance is approximately equal to the actual torquer dc resistance. When no torquer current is needed, the "dummy" is energized by the PTE torque-no torque logic (Fig. 2.8). This transfer provides a constant load to the current source. It also provides a thermal input to the gyro equivalent to that seen by the gyro when torquing is commanded. This action minimizes thermal transients in the gyro by providing constant power regardless of torquing requirements.

6. Bandpass Preamplifier

This preamplifier provides the necessary gain to raise the level of the gyro SG error signal to be compatible with the PTE input circuit; it also provides bandpass filtering to minimize the unwanted 800 Hz components induced by the gyro wheel excitation. An adjustment is incorporated to correct the phasing of the SG signal so that it matches the timing of the interrogate pulse. See Fig. 2.6. The schematic drawing number is 2304030.

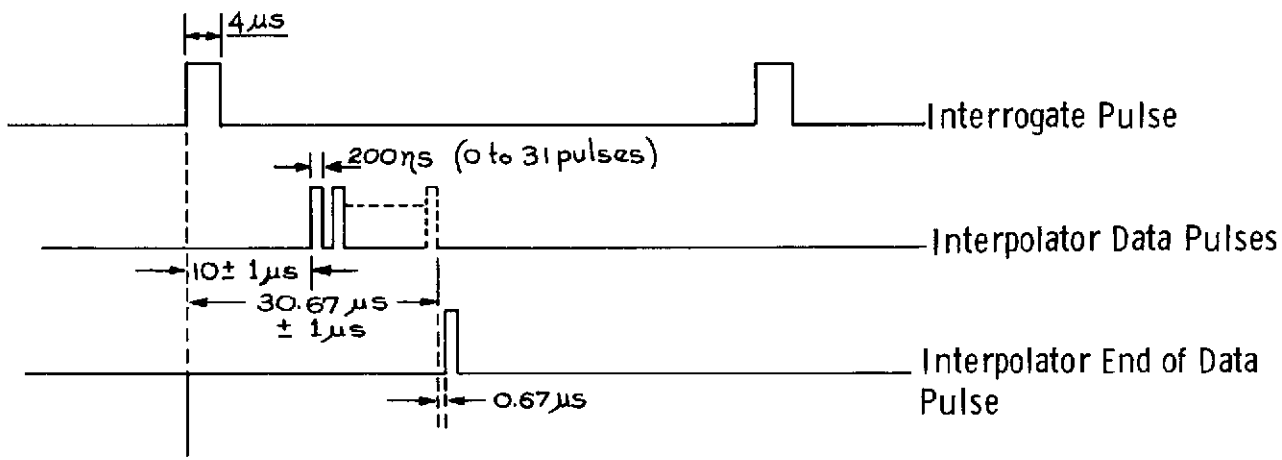

A) $+\Delta\theta$ (+5 Vdc amplitude, 2 μsec wide)

B) $-\Delta\theta$ (+5 Vdc amplitude, 2 μsec wide)

C) Interpolator Data Pulses. 4.5 Vdc, 0 to 31 pulses at 1.5 mc rate

D) Interpolator End of Data Pulse. 4.5 Vdc, 200 nsec pulse width, 208.33 μsec repetition rate

Fig. 2.11 SIRU Gyro Module Electrical Interface Output Signal Requirements

Torquer Tuning Network

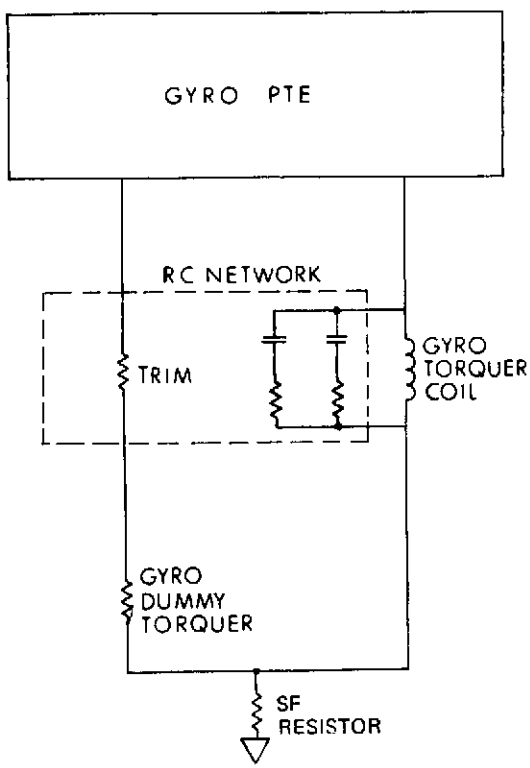

Fig. 2.12 Gyro Module RC Network

7. Temperature Controller

The function of this unit is to minimize temperature sensitive gyro drift terms by maintaining the gyro temperature constant within ± 0.1°F over a range of ambient temperatures, wheel power variations, and other thermal disturbances. The controller contains two legs of a dc resistance bridge; the other two legs being temperature sensitive resistors located in the gyro. The bridge is balanced at the operating temperature (132°F) of the gyro. Any deviation from this temperature unbalances the bridge and generates an error voltage. This error is then amplified by a low level, high gain, dc, integrated circuit operational amplifier. This amplifier contains an integrated circuit temperature control loop which keeps the dc amplifier circuit at constant temperature in order to minimize dc drift due to temperature variations within the amplifier. This amplifier then drives another integrated circuit operational amplifier which provides current to the base of the power output transistors which in turn deliver power to a heater located on the gyro (See Fig. 2.2). The power transistors are assembled into the gyro end mounts so that the power dissipated in the power transistor is transferred to the gyro. Since the controller is essentially a series dc proportional regulator, the sum of the power dissipated in the transistor and the power dissipated in the gyro heaters is linearly proportional to the gyro heater current. This mechanization is in contrast to the usual situation where the power transistor is located at some distance from the gyro so that the gyro sees only the heater power which is proportional to the square of the heater current. This linear operation makes dynamic compensation of the control loop easier and provides for maximum thermal efficiency of the controller output circuitry. Dynamic loop compensation is achieved by the use of a series of RC networks connected between the emitter of the TG end mount power transistor and the input to the high gain amplifier. The time constant and gain of the RC network are chosen so as to stabilize the control loop which would otherwise be unstable due to the high loop gain and the thermal lags between the heater and sensor. The network also optimizes the transient response to thermal disturbances. The schematic drawing number is 2304058.

Gyro Temperature Control Circuit

The gyro temperature control circuit is similar to the accelerometer temperature control circuit described in Volume IV with few exceptions. It consists of a safety thermostat, a proportional temperature control module, power transistors, heaters and sensors. See Fig. 2.13.

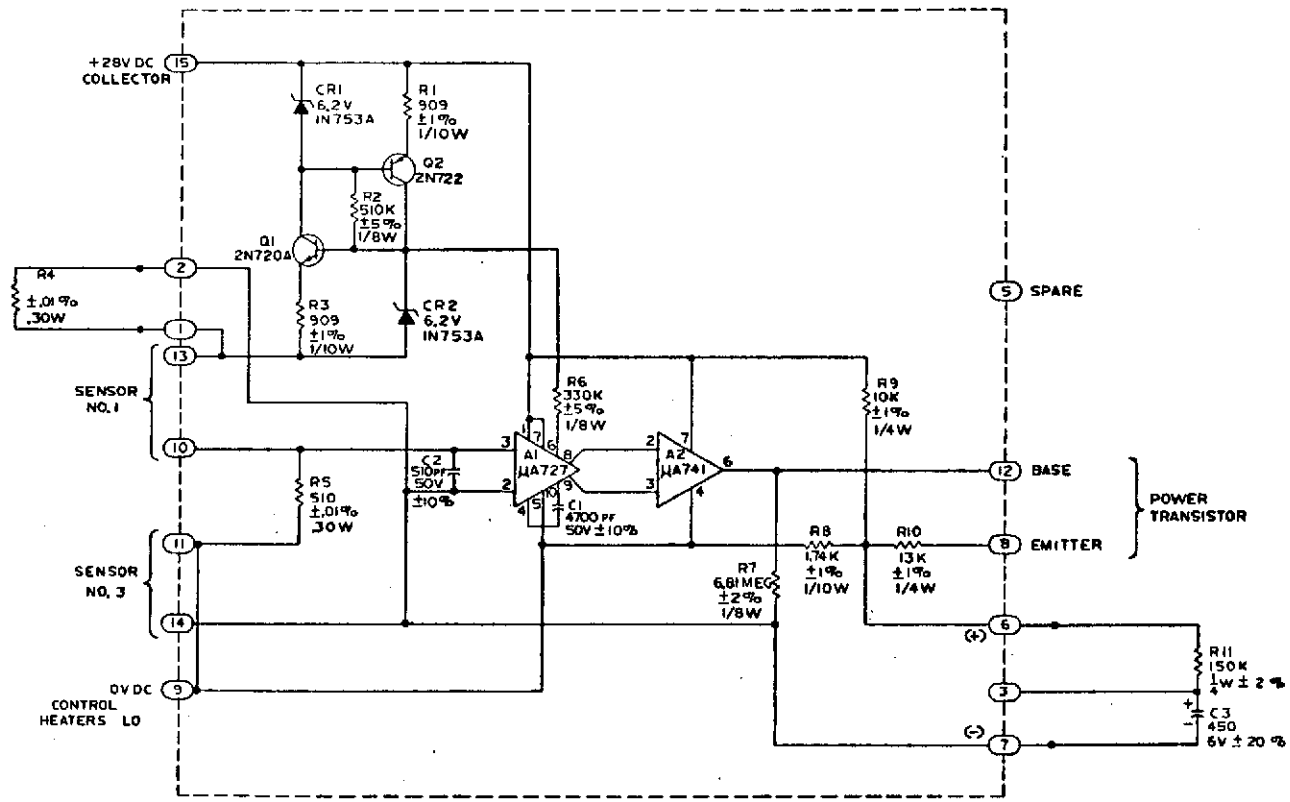

Fig. 2.13 Gyro Temperature Controller Schematic

The safety thermostat is mounted on the base plate. It opens at 147±3°F and closes at 132°F min. The proportional temperature control module circuit is the same as the one for the accelerometer module except that the amplifier uses different values for feedback compensation and has a temperature sensor in the feedback circuit. The two power transistors are designed to screw into the gyro end mount assemblies. The control heaters are also mounted on the end mounts. Thus, the power dissipated in the control transistors assists in heating the gyro. Interwoven with the control heaters are the GSE heaters and sensor used to provide standby control. The control heaters each dissipate a maximum of 5.2 watts for a total of 10.4 watts (max) control power. The sensor circuit is padded to control at a nominal temperature of 130±0.25°F. Control accuracy is ±0.1°F.

Table 2.4 is a summary of gyro module temperature control parameters.

Table 2.4
Gyro Module Temperature Control Parameters

Voltage	28 vdc Unregulated
Heater Power	10.5 watt max @ 21.5 vdc
Power Transistor	SCD 2304307
Control Heater Resistance	80 ohms
GSE Heater Resistance	140 ohms
Control Sensor Resistance	510 ohms @ 130°F
Monitor Sensor Resistance	500 ohms @ 130°F
GSE Sensor Resistance	510 ohms @ 130°F
Sensors Temp Coefficient	+0.00226 ohms/ohm/°F
Gyro Nominal Temperature	130°F ± 1°F
Gyro Temp Control Accuracy	±0.1°F

8. Normalization Assembly

All of the components necessary to normalize the various gyro parameters are located in this assembly. These parameters are the gyro temperature sensor resistance, the signal generator phase shift, the suspension "Q", the suspension stiffness and the signal generator quadrature. In addition, the two resistors used for suspension current monitoring are located in this module. Components for this module are selected during the appropriate phases of gyro and gyro module testing. The schematic drawing for this module is 2304093.

The location of the previously described components in an assembled gyro module is shown in Fig. 2.2. The module is constructed in sections to simplify assembly, maintenance and repair. These subassemblies are shown in Fig. 2.14. This figure also shows a fully assembled module (lower left) and a covered module (upper center).

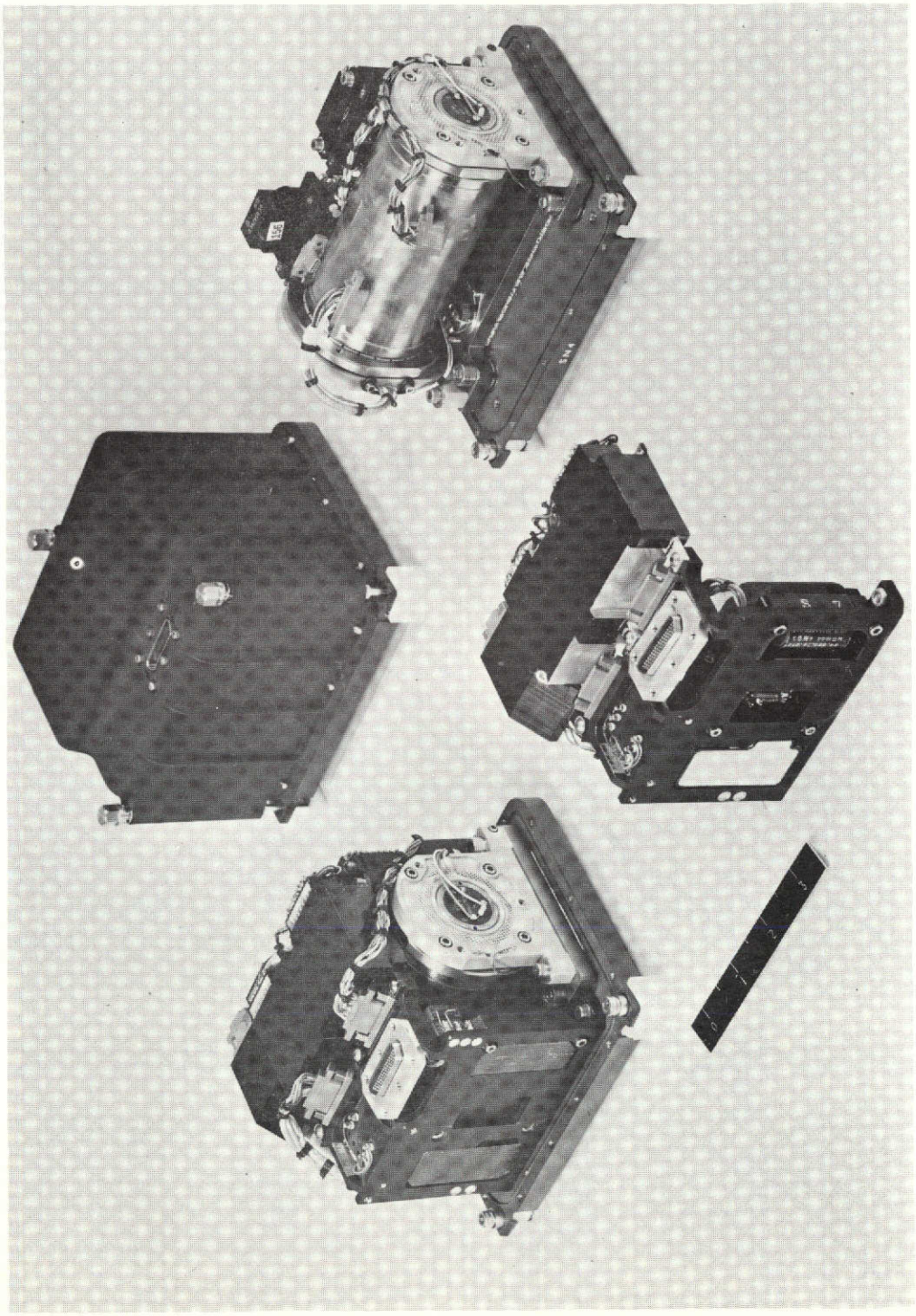

Fig. 2.14 Gyro Module

3.0 Gyroscope Instrument Status

The gyroscope employed in the SIRU program is the MIT/CSDL designed 18 IRIG Mod B. The development of this instrument as the 18 PIRIG started in 1963 under the sponsorship of NASA/MSC as part of the effort to define the fundamental requirements for a strapdown Guidance, Navigation and Control (GNC) system. This program has been previously identified in the Historical Background section of Chapter 1, Volume I. The 18 PIRIG was the first CSDL gyro built specifically for strapdown application. It employed a ball bearing wheel and a permanent magnet torquer sized to provide a 30^{o}/sec rate input. It was used on a strapdown experimental system built for the Navy by the Charles Stark Draper Laboratory (CSDL) in 1964.

The 18 IRIG Mod B was developed under NASA/MSC sponsorship for use on contract NAS 9-6823, Structure Mounted Studies (SMARTS). See CSDL report R-600, Volume IV, for a complete report of all effort expended and the results obtained in the basic preparatory program. Four 18 IRIG Mod B gyros (designated as the 410 series) were fabricated under the SMARTS program. Improvements were incorporated in these gyros over the production period, constrained by hardware availability and delivery requirements. These improvements are identified as:

1) Introduction of a composite magnetic structure for the PMT stator permitting an accurately located flux density distribution and resulting in a reduction in the torque sensitivities due to rotational, radial and axial float motion
2) Reduction of PMT stator to suspension rotor coupling by the introduction of a sleeve of magnetic material between the two elements
3) Reduction of stop-bias hysteresis by use of low iron content beryllium for the torquer coil holder (further improvements were incorporated in succeeding production)
4) Optimization of the gas bearing design to improve slew capability and stop-start wear.

A second group of 18 IRIG Mod B gyros were produced at CSDL specifically for the SIRU program. These instruments were identified as the 420 series and included the design improvements suggested by the results on the earlier units and by on-going developments under other gyro programs. These improvements were:

1) Reduction of 800 Hz motor frequency pickup by rerouting wiring within the gyro

2) Elimination of magnetic material in the glass to metal seal terminal strips in the SG end housings within the gyro
3) Reduction of both eddy current effects and stop-bias hysteresis by the introduction of a Beryllium Oxide (BeO) torquer coil support
4) Substitution of Armco soft iron with Hypernik for the torquer return path to further reduce eddy current effects
5) Improved magnetic shielding to further reduce the PMT stator to suspension rotor coupling by both material and dimensional (thickness) changes
6) Further improvements and refinements of the gas bearing wheel design to reduce the gyro sensitivity to cooldown and to provide a better compliance match

A total of 13 series 420 gyros were delivered for system use. A final report covering this development and production program is identified as CSDL Report R-664. Areas of desirable further improvement were identified at this stage as

1) Increase slew rate capability
2) Further improvement in compliance match
3) Reduce the anisoinertia mismatch

Specific deficiencies are identified as increasing starting voltage requirement with life and g-sensitive bias shifts across cooldowns.

The 13 gyros provided by the program described above have been operating in the SIRU gyro laboratory and system for a total period of 34 calendar months through December, 1972, accumulating a total of 155,400 operating hours, 116,400 of these being in system operation. A total of 1919 stop-starts were recorded during that time. The operating hours accumulated for several gyros exceeded 19,000 hours. Gyro failures during the 23,300 hours of system operations were two; one a wheel failure and one a float freedom/contamination failure. The resulting observed MTBF is therefore 58,200 hours and at the 90% confidence level is 22,000 hours.

Since completion of the series 420 gyros, efforts to further improve the performance, operating characteristics, and the producibility aspects of the size 18 strapdown gyro have continued under Navy sponsorship. This development program attacked the two outstanding deficiencies noted above. To improve the starting load characteristics, the bearing material was changed to BeO from the alumina ceramic previously used. It has the advantage that no lubricating film is required and the crowned configuration is not necessary. Test results for the new bearing show

that 100,000 stop-start cycles are obtained (corresponding to a two volt increase in starting voltage specification) compared to the 15,000 stop-start cycles (corresponding to a six volt increase in starting voltage specification) for the previous bearing. The BeO wheels have withstood high speed touchdowns whereas the alumina wheel has suffered catastrophic failure under this condition.

In the new instrument series, identified as Mod D, the change in wheel material is combined with an integral BeO gimbal assembly designed with no float balance adjusters or other asymmetrical appendages. A more rigid torquer coil mounting cylinder is integral with the gimbal structure. This configuration has understandably resulted in substantial improvement in the g-sensitive drift shifts across cooldowns; from 0.3°/Hr/g peak to 0.03°/Hr/g peak in component laboratory tests at CSDL. Producibility is improved by the attendent reduction in the number of individual parts required to assemble a gyro; from 86 for the Mod B to 40 for the permanent magnet torquer Mod D.

4.0 Gyro Module Performance

Complete records of the test results obtained on the gyros both in and out of modules are maintained. Gyro testing is performed in the gyro laboratory as described in Section 5 of this volume and gyro module performance is measured during operation of the SIRU system as described in Volume I.

The data from these records are analyzed periodically to provide a statistical measure of the performance achieved. Figure 4.1 presents scale factor rate linearity test data measured in both the component and system labs. That data shows a scale factor difference between the two labs of approximately 150 ppm. Investigation revealed that the SF magnitude was sensitive to variations in the level of the 40v excitation between the component area and the system test area.

Tests were conducted with several pulse torque electronics (PTE) modules and SIRU gyro module #10 to evaluate

1) DC amplifier circuit stability
2) Scale factor sensitivity to 40v dc supply variations
3) Scale factor stability
4) Scale factor linearity
5) Scale factor sensitivity to RC network tuning

Modification of the dc amplifier compensation, combined with an increase in the padded resistance of the torquer circuit and resistive tuning of the torquer circuit, has proven successful in desensitizing the SF to variations in the 40v excitation. Tests with a modified module have demonstrated a significant improvement, the delta SF between module and system tests was reduced to a maximum of 13 ppm.

Table 4.1 presents a summary of gyro module calibration data at system delivery. This table shows that pulse torque scale factor magnitude can be set to within 250 ppm of nominal, rate linearity is better than 50 ppm, and alignments of better than 20 $\widehat{sec}$ are obtained.

Figures 4.2 and 4.3 summarize stabilities of bias drift (NBD), g-sensitive drifts (ADSRA, ADIA and ADOA), g^2 or compliance drift, scale factor (SF) and input axis alignments obtained across remounting, cooldowns and test repetition.

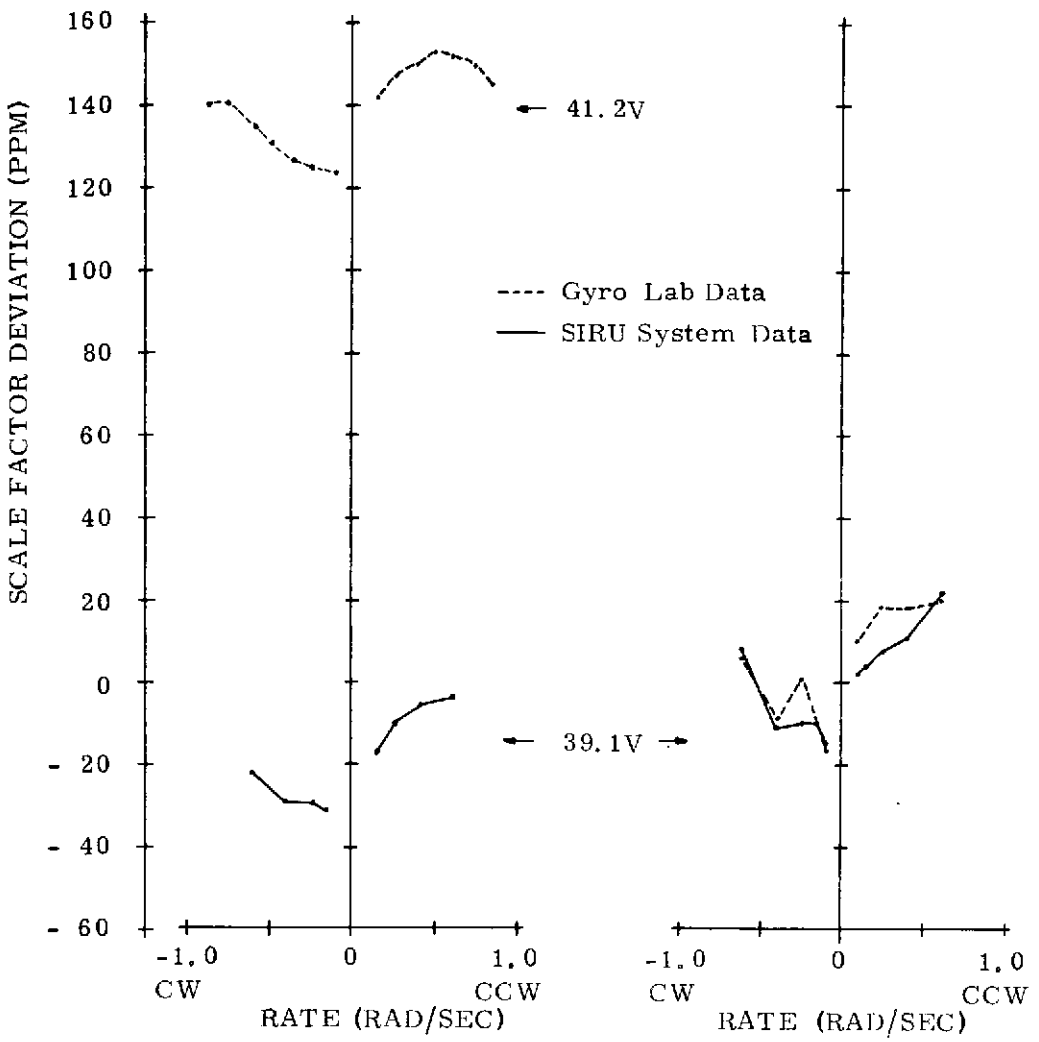

Fig. 4.1 Scale Factor Sensitivity to Variations in the 40V Excitiation

Table 4.1

Component SIRU Module Data (Post-Interpolator/Compensator Retrofit)

SIRU Mod. S/N	SIRU Mod. Axis	Gyro S/N	Scale Factor (ppm) Linearity[1] CW	Linearity[1] CCW	Magnitude From Nominal +SF	Magnitude From Nominal -SF	Align.[2] OA	Align.[2] SRA
2	C	425	35	15	105	101	6*	-4*
3		423B	18	27	99	107	-20	10
4	F	420A	17	15	124	143	38	-20
5A	D	428B	50	50	205	241	-	-
6B	E	421	51	31	90	92	-60	-65
7	A	424A	41	35	78	70	-21 -33	-53 34
8	B	426A	14	22	85	67	(-1)*	(18)*
10		430B	49	39	226	235	32	7

Note : 1. Scale Factor : Linearity (1/16 to 1 radian), +SF at 1/8 radian.

2. Alignment in arc seconds.

*Alignments using precision procedure, other alignments are preliminary.

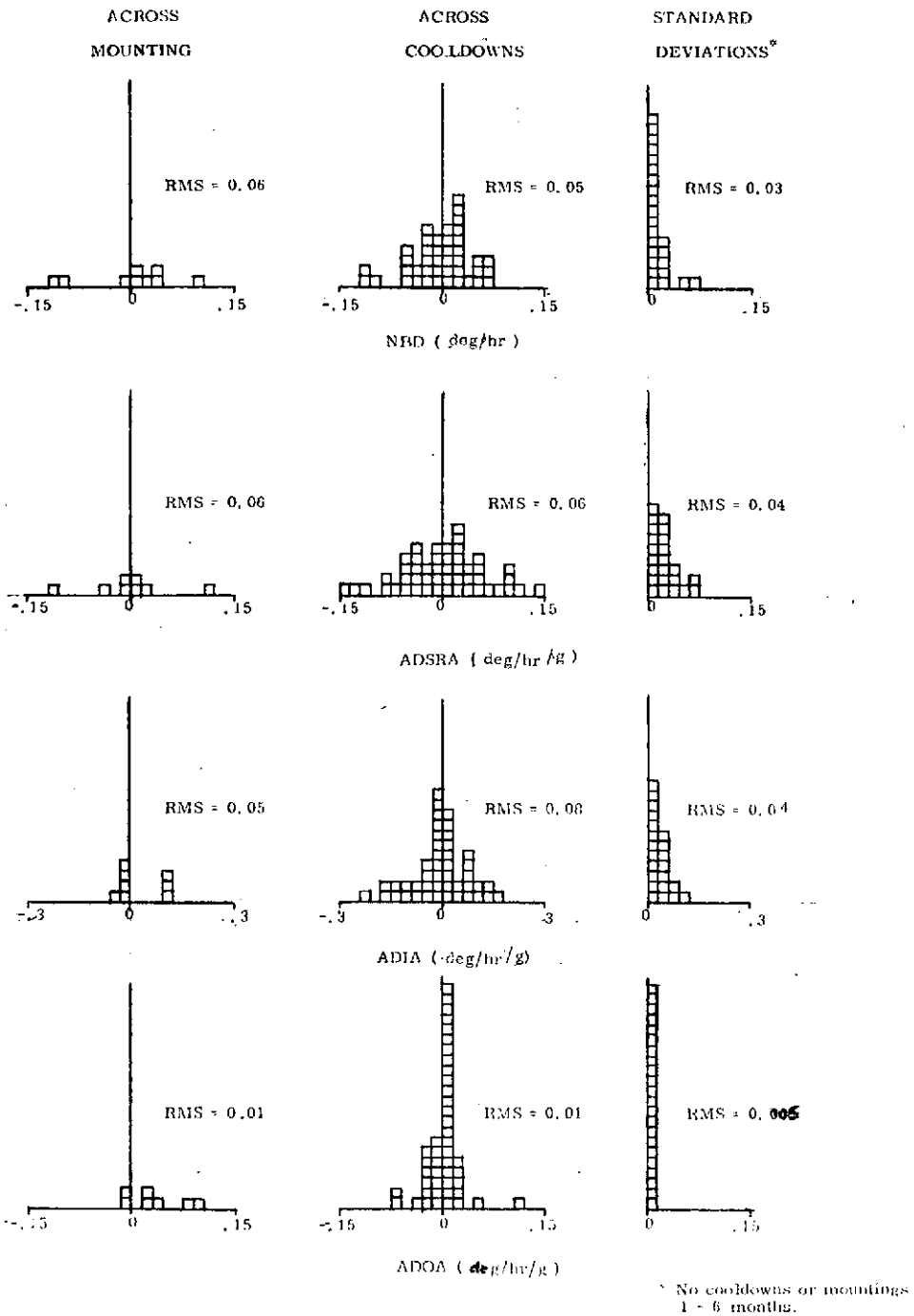

Fig. 4.2 Gyro Drift Performance
18 IRIG Mod B

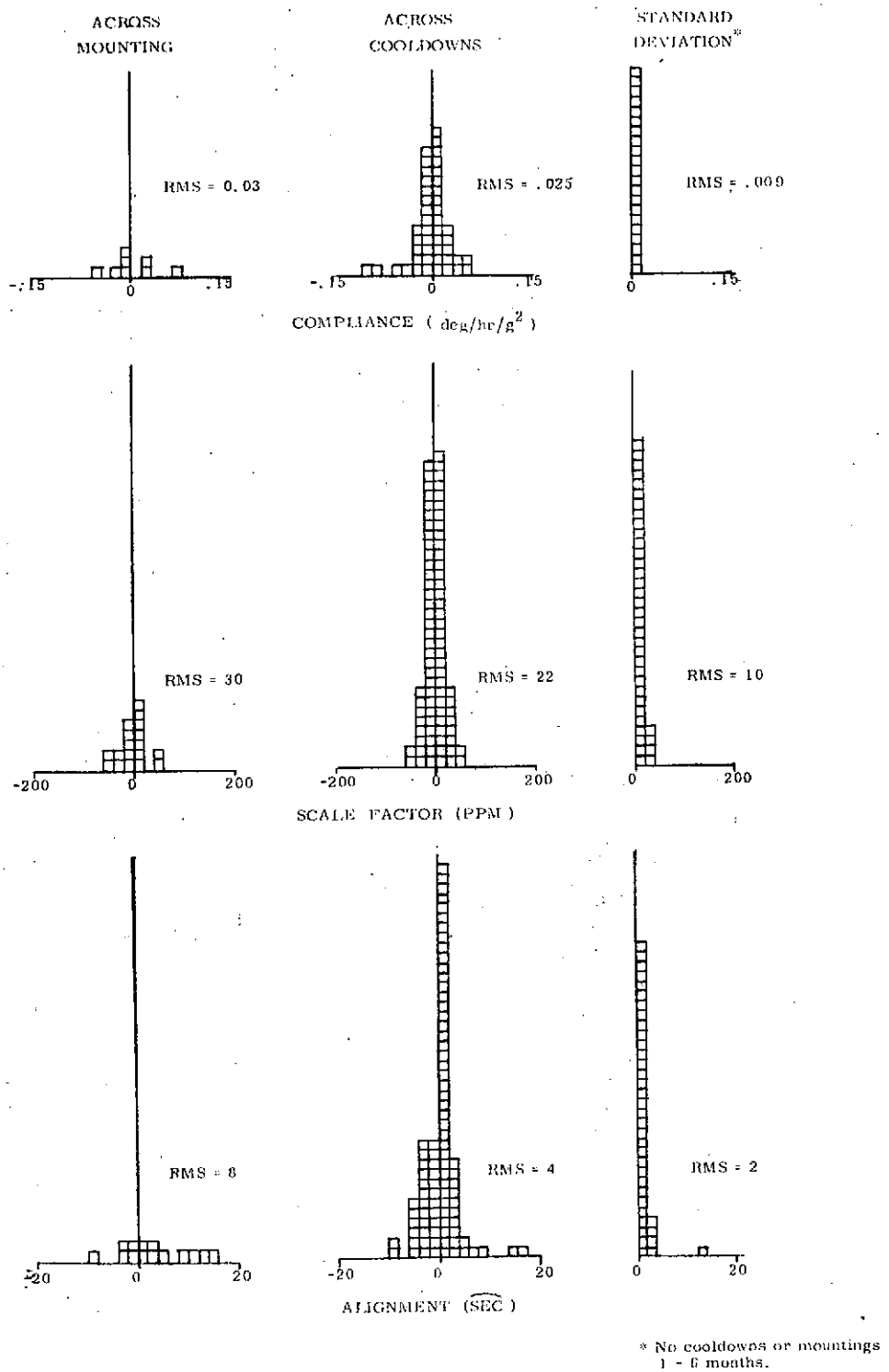

Fig. 4.3 Gyro Compliance, Scale Factor, and Alignment Data 18 IRIG Mod B

The delta drift, or change in drift magnitude, alignment and SF has been tabulated and an rms calculated for the sample size to show the effect of module remounting (Column 1) and of system cooldowns (Column 2). The larger sample size of cooldown data results because all installed instruments are affected by a system cooldown whereas remounting affects only individual instruments.

A comparison of the g-sensitive drift for these two cases show nearly identical performance; that is, both the spread in delta magnitudes and the calculated rms values for each term are similar. This is to be expected, as the environmental impact on the instrument is nearly the same in each case (all power off). There is no apparent effect from the physical movement of the module during remounting. This g-sensitive drift change across cooldown is a deficiency of the 18 IRIG Mod B gyro population used in SIRU. An improved instrument, the 18 IRIG Mod D, with a redesigned integral wheel and gimbal (described above) has substantially reduced this sensitivity. The equivalent performance of the Mod D across cooldowns is documented to be on the order of $.015^{\circ}$/hr.

The tabulations of standard deviations (Column 3) for the various terms are derived from one to six months of calibration test results chosen to exclude all interposing cooldowns or remounts. This data is considered to be representative of performance across cooldowns expected with the incorporation of the 18 IRIG Mod D or an equivalent instrument.

SF and alignment stability performance, for all three cases, is very respectable, and the standard deviations are indicative of the stability of the hardware and the sensitivity or resolution of the calibration and data reduction process. As explained in subsequent sections, reductions in SF differences across mounting have been achieved through implementation of hardware modifications, and reductions in alignment differences across mounting can be achieved through the use of an optical calibration fixture.

Table 4.2 shows the average sigma of the drift stability applicable to each instrument in five of the test positions shown in Fig. 4.4. This data was derived from overnight and weekend test runs of approximately 16 hours to 60 hours duration. Statistically the system performance is seen to be relatively unaffected by position with respect to gravity.

Table 4.2
Average Sigma of the SIRU System Overnight
Stability Data (Gyros)

AXIS	GYRO	POS #1	N	POS #2	N	POS #3	N	POS #4	N	POS #6	N
A	MB-424A	6.08	7	6.06	11	1.98	3	2.97	3	3.16	6
B	MB-426A	9.39	7	8.68	10	5.67	3	1.78	4	3.06	7
C	MB-425	3.41	7	2.88	10	6.72	3	7.48	3	2.31	5
D	MB-428B	3.42	1	2.91	2	——	-	4.35	1	——	-
E	MB-421	6.00	4	4.20	9	3.48	3	2.49	1	5.31	4
F	MB-420A	3.14	6	2.43	9	2.02	3	1.71	3	3.90	7

Values in deg per hour x 10^{-3}

Figs. 4.5 through 4.10 provide a continuous record of the gyro parameters for each module over an extended period of testing. As previously discussed, the g-sensitive drift changes that occurred across cooldown are a design deficiency for this instrument which was resolved with the change to the 18 IRIG Mod D configuration.

The following three figures, 4.11 - 4.13, are typical drift stability tests measured in the pulse torque-to-balance mode. As described below, the figures show a decrease in stability with increasing proportions of g-sensitive drift, especially ADIA.

In Fig. 4.11 the instrument module is oriented with its output axis down sensing approximately 4 ^{o}/hr of earth rate and exhibiting essentially its bias drift magnitude and stability. The 60 hour torque-to-balance test data have a standard deviation of .001^{o}/hr.

In Fig. 4.12 the instrument module is sensing the horizontal component of earth rate and exhibits its combined bias and ADSRA drift magnitude and stability. This gyro laboratory 12 hour test shows a standard deviation of .0016^{o}/hr.

In Fig. 4.13 the instrument is aligned approximately parallel to the earth rotation vector sensing full negative earth rate and exhibiting its combined gyro bias, ADSRA and ADIA drift magnitudes and stabilities. The standard deviation of the 60 hour test is .006^{o}/hr.

Each data point in Fig. 4.14 is obtained from 50 revolutions of the test table. With the loop quantization of approximately .44 sec/pulse, the one pulse resolution ia equivalent to 0.7ppm. The data shown, therfore, all lies within a 3 pulse bandwidth.

RA1 = ROT. Axis 32" Table
RA2 = ROT. Axis 16" Table
TA1 = TRUN. Axis 32" Table
TA2 = TRUN. Axis 16" Table

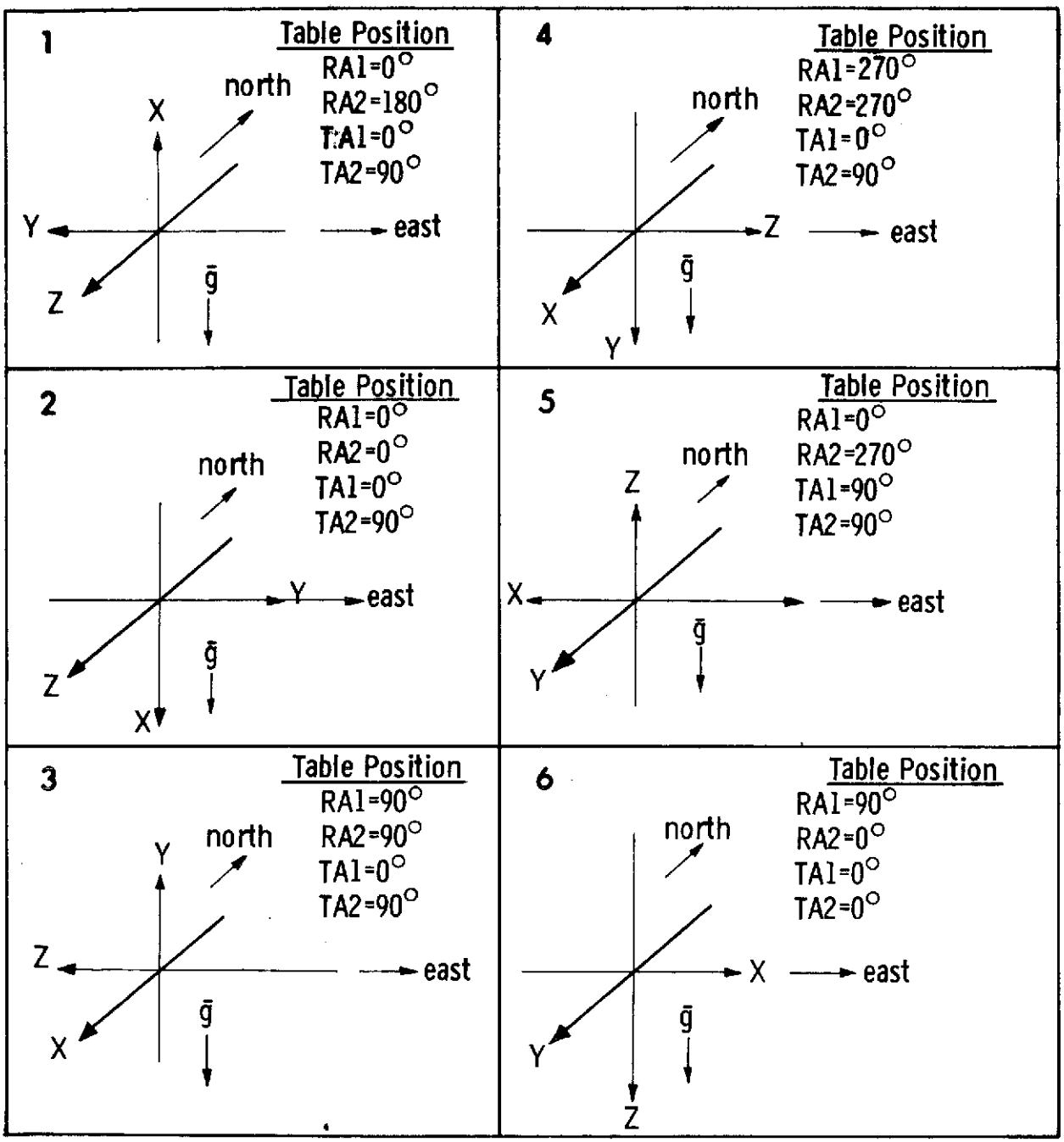

Note : Positions 2, 4 & 6 are the Basic Positions for Rate Testing

Fig. 4.4 Calibrate Alignment Positions

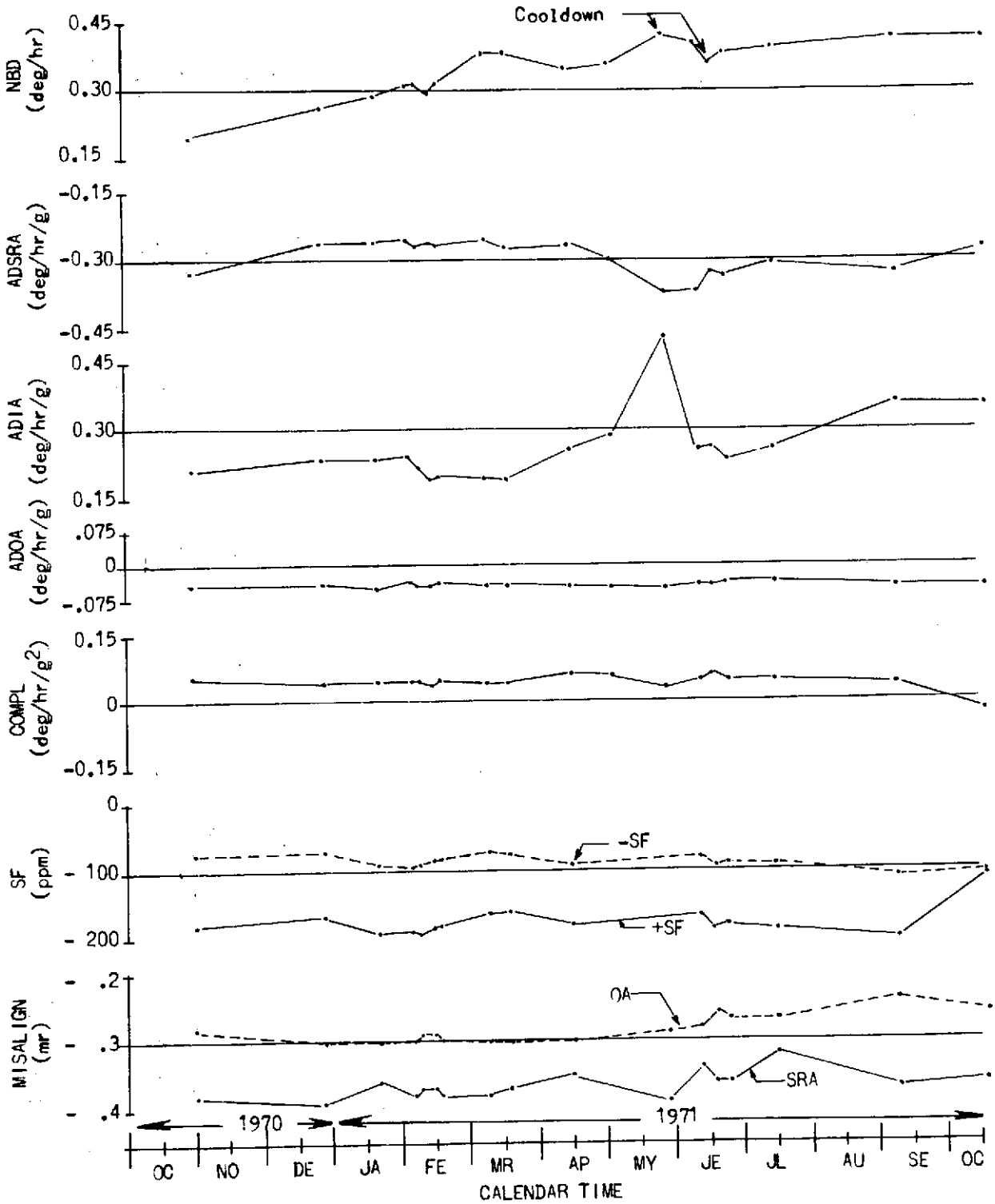

Fig. 4.5 Performance Data vs Calendar Time, A Axis

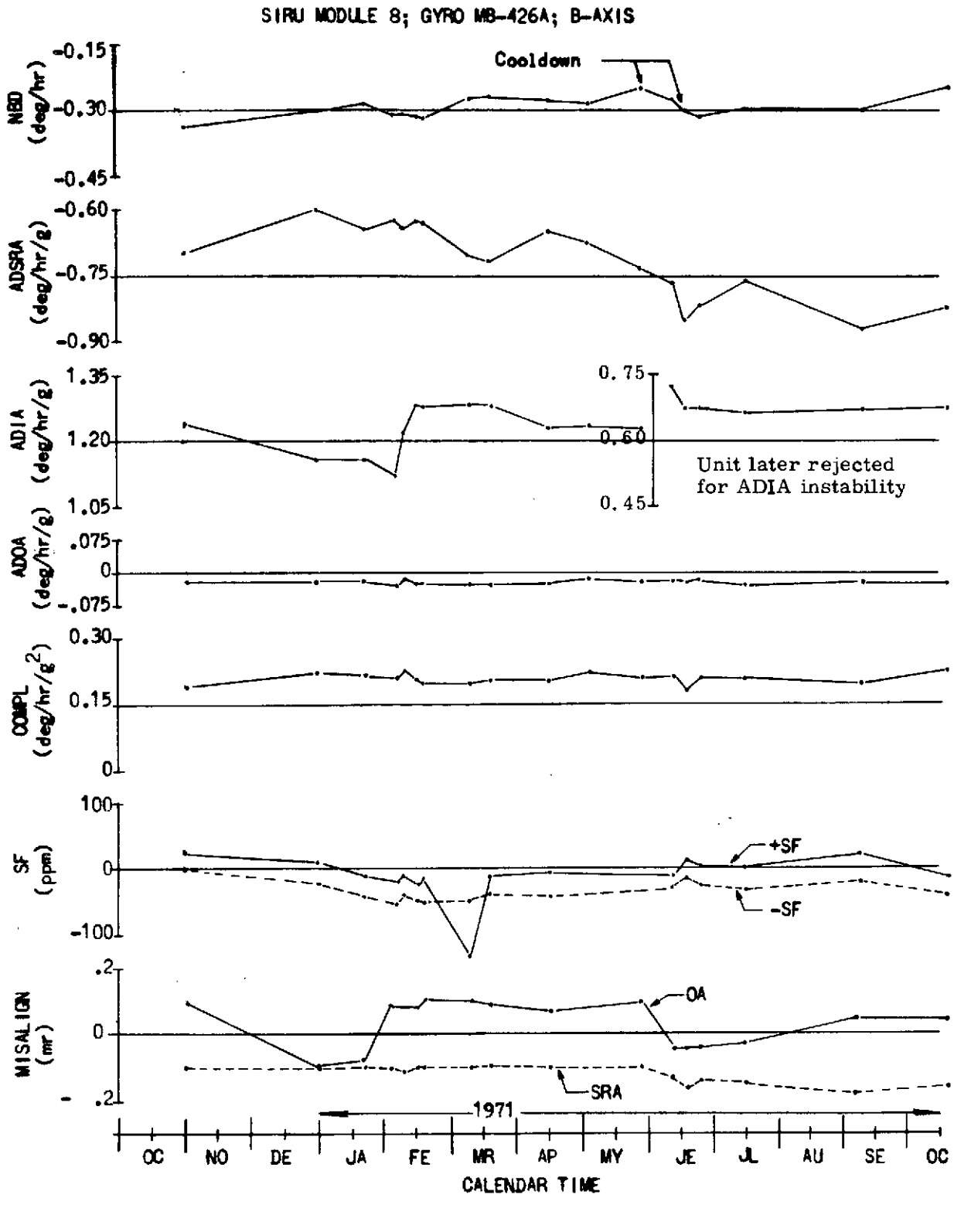

Fig. 4.6 Performance Data vs Calendar Time, B Axis

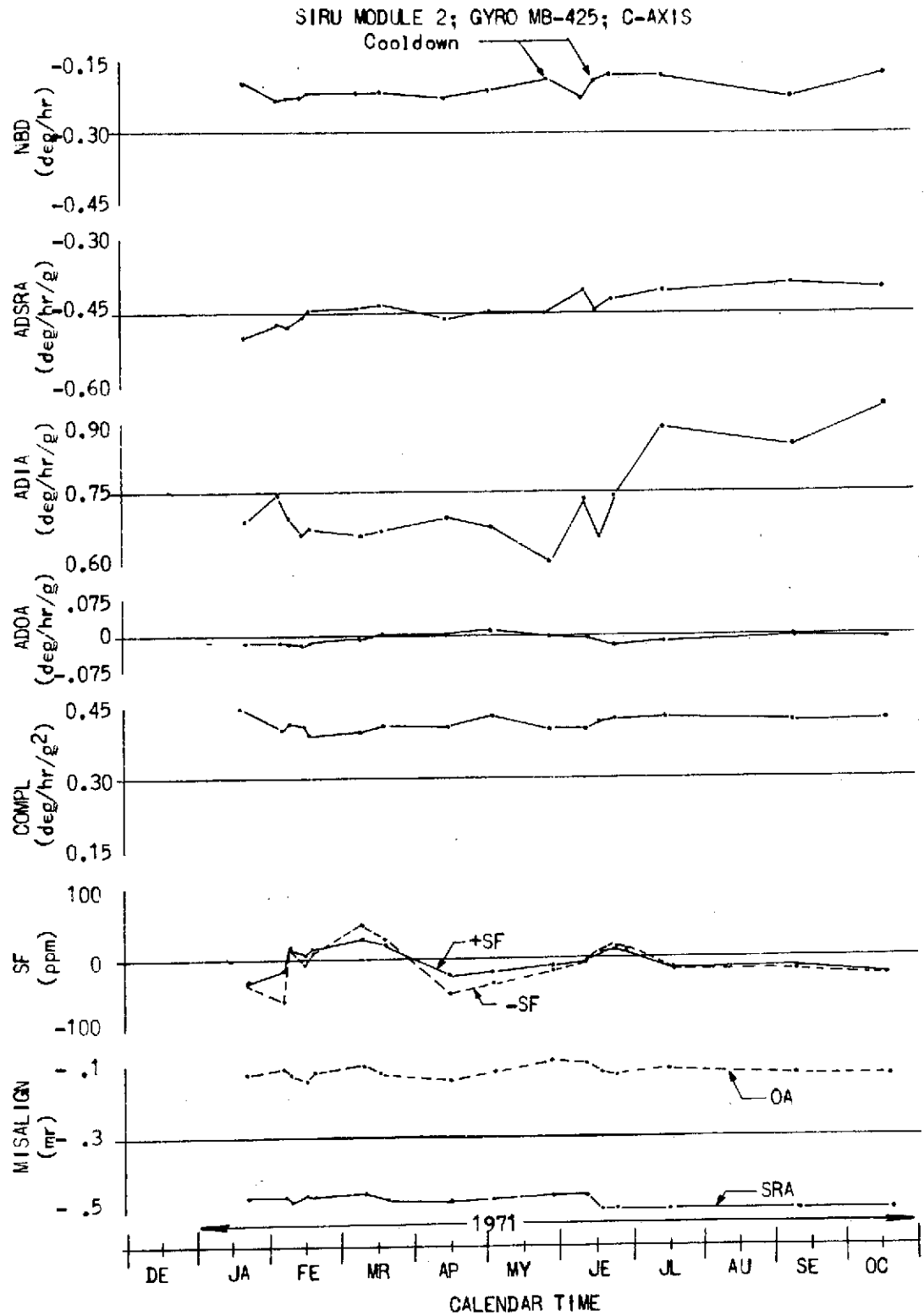

Fig. 4.7 Performance Data vs Calendar Time, C Axis

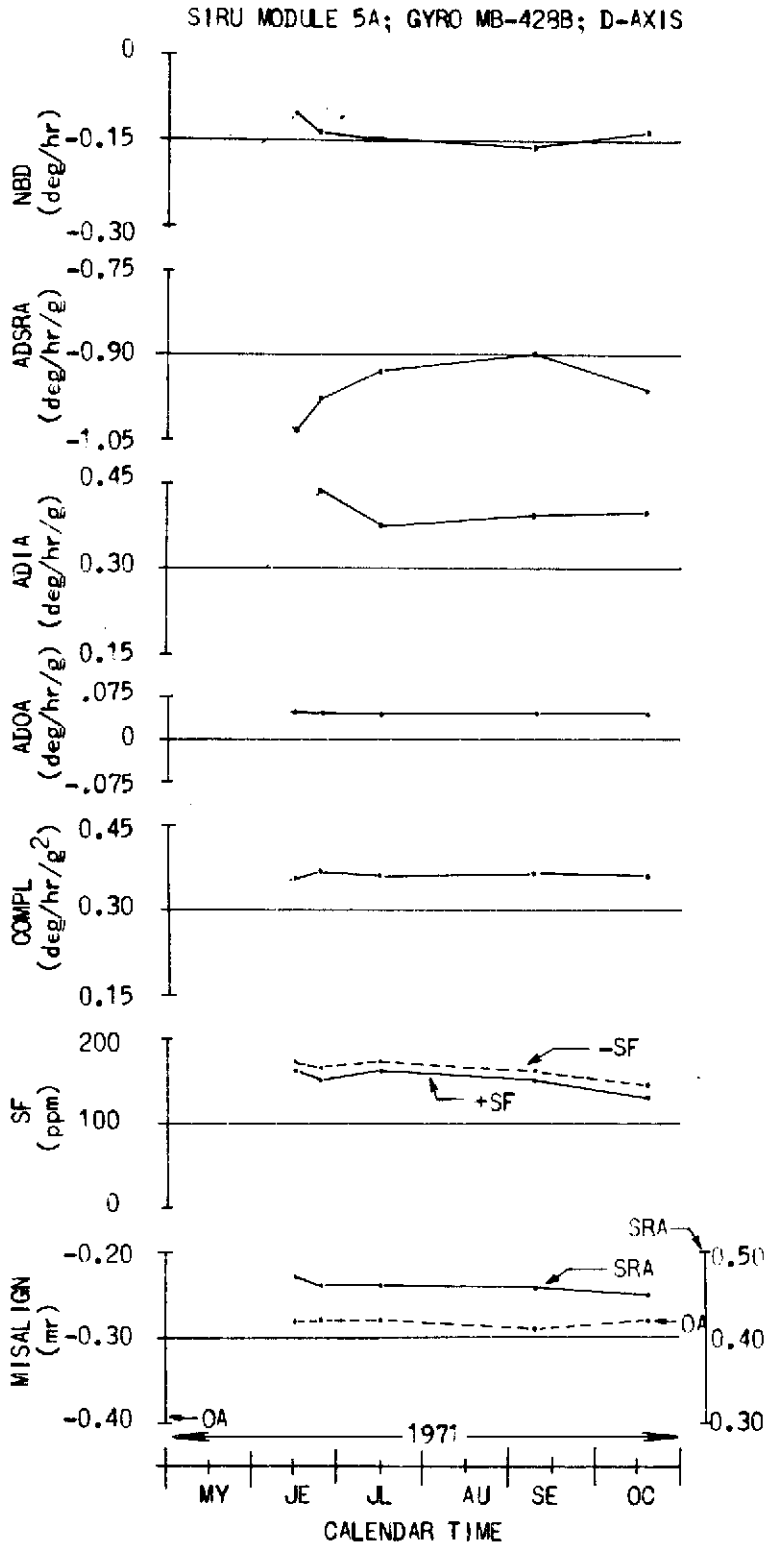

Fig. 4.8 Performance Data vs Calendar Time, D Axis

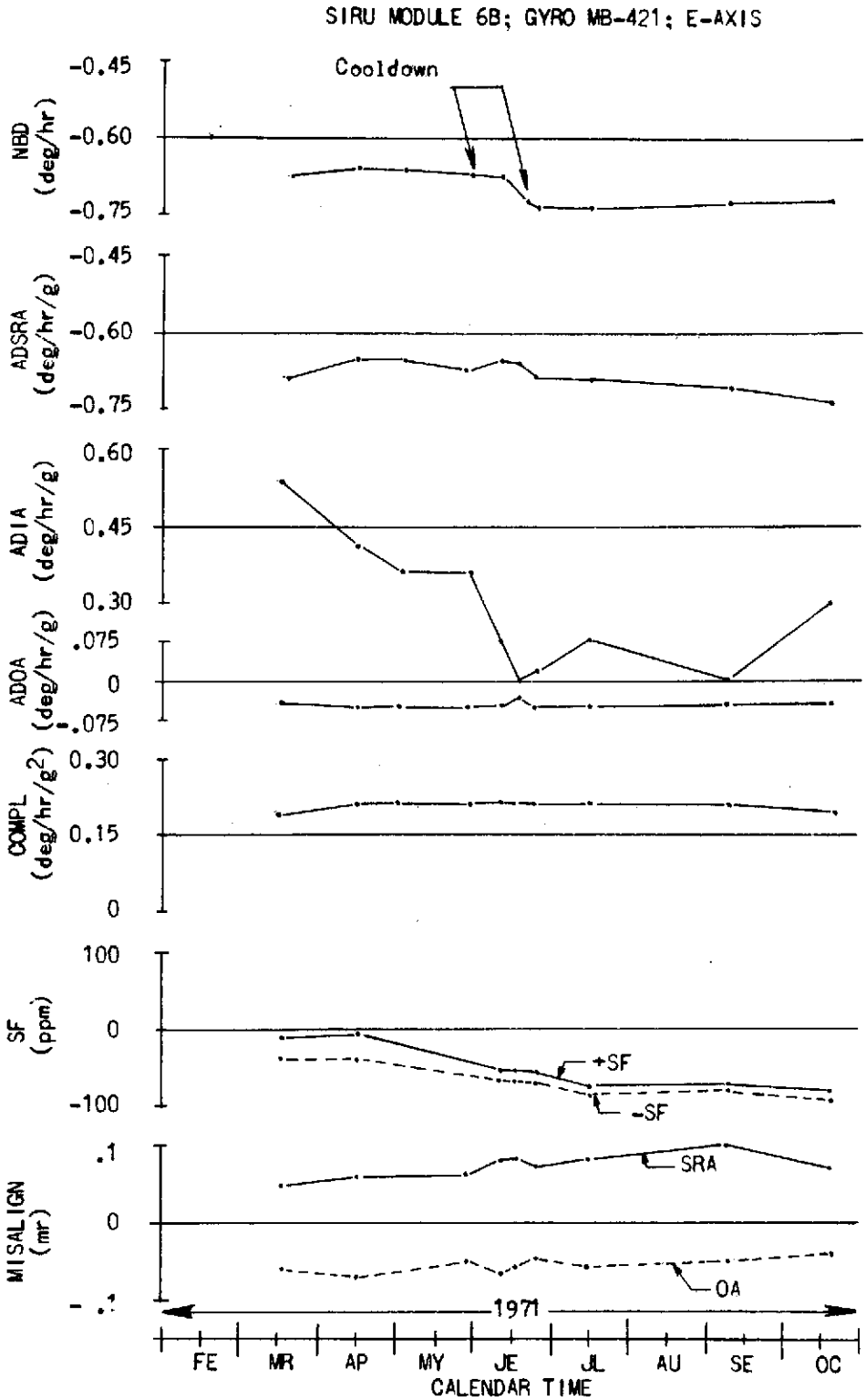

Fig. 2.9 Performance Data vs Calendar Time, E Axis

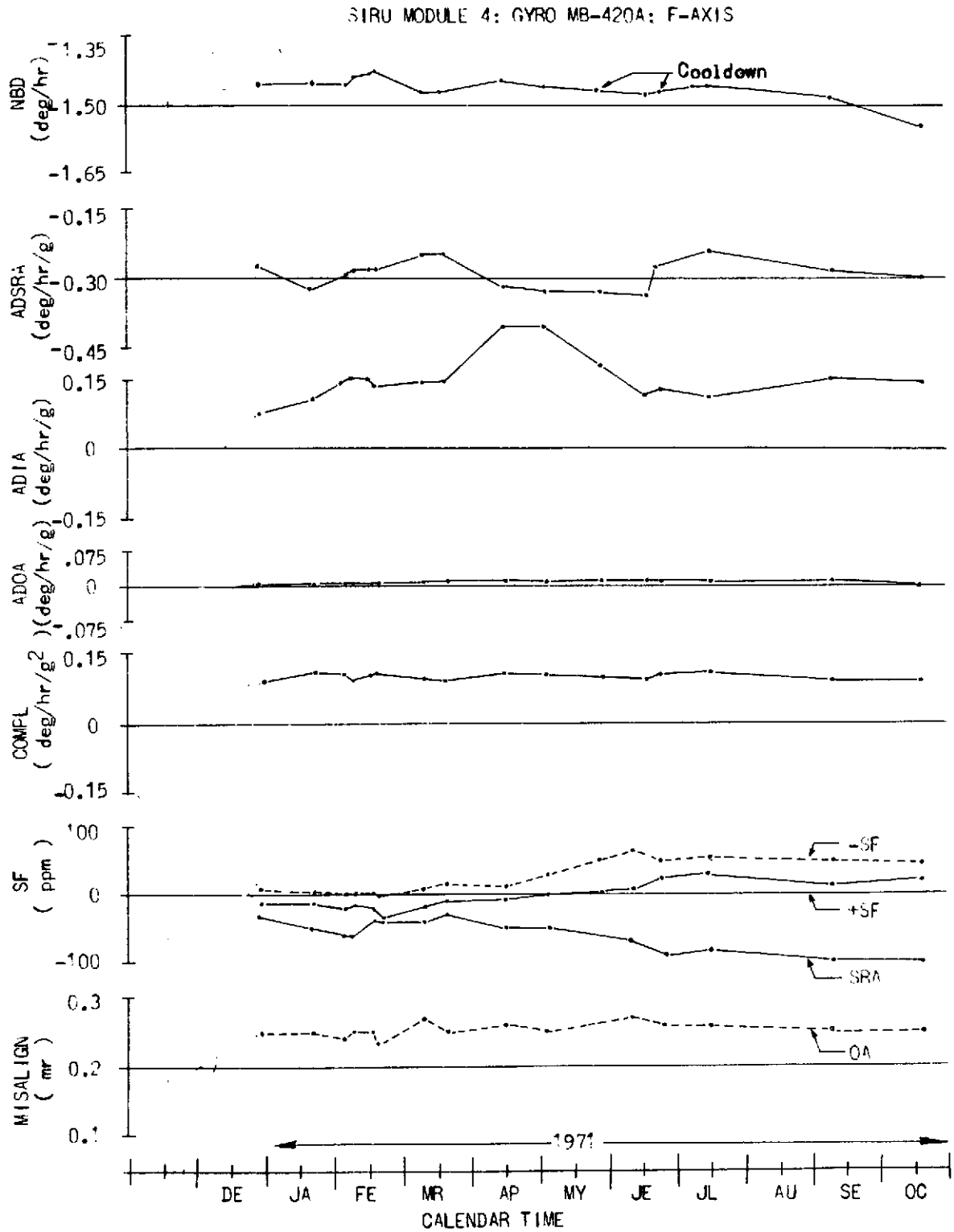

Fig. 4.10 Performance Data vs Calendar Time, F Axis

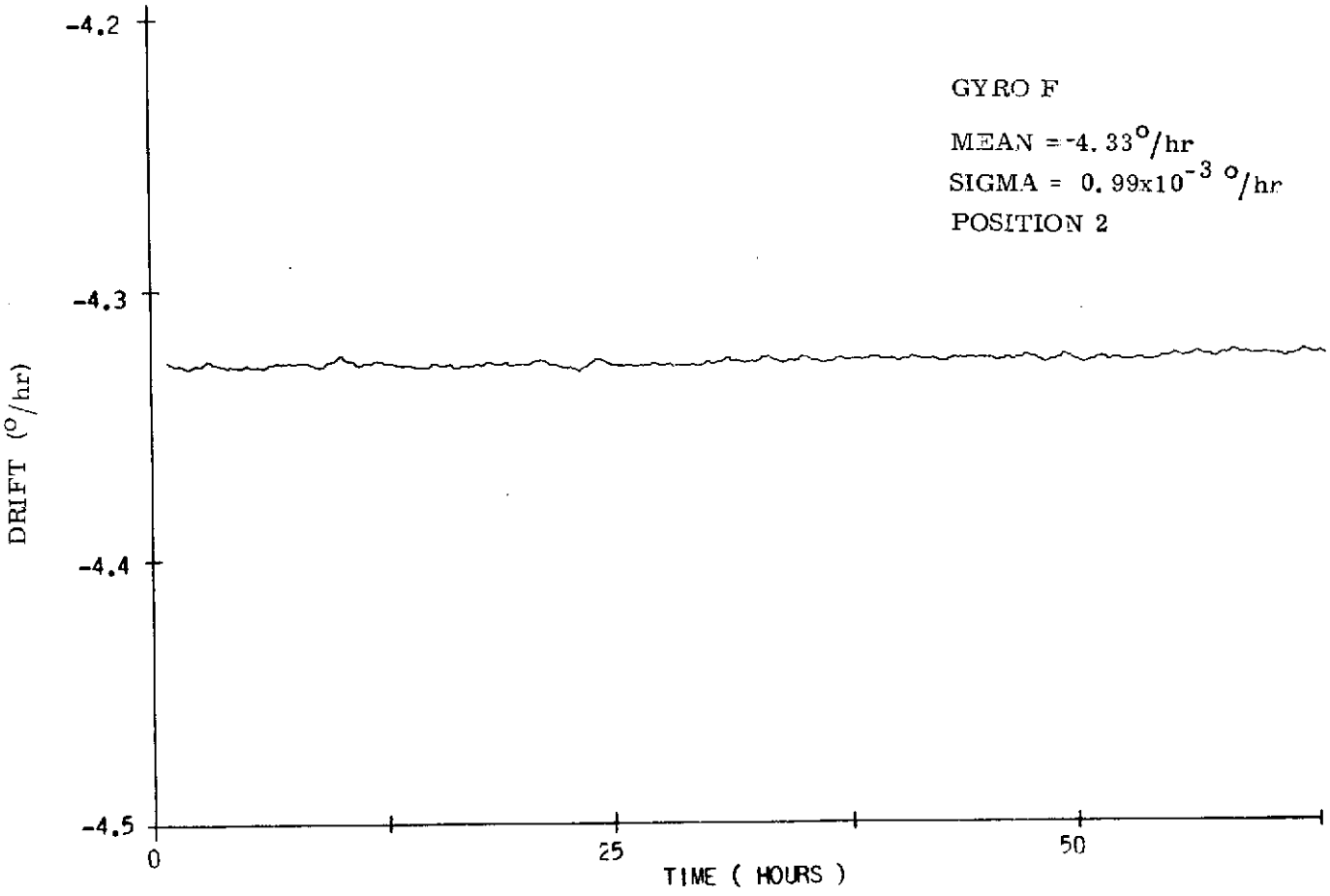

Fig. 4.11 Fixed Position Gyro Drift Stability

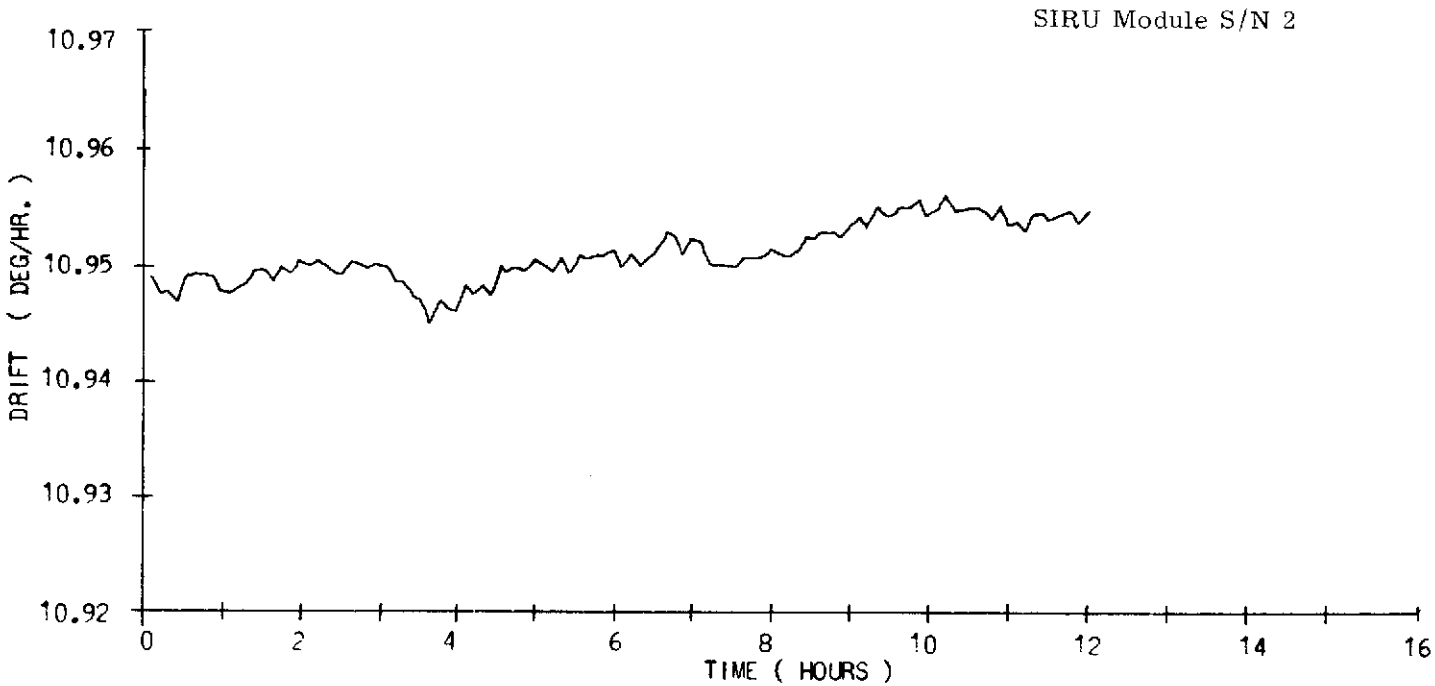

Fig. 4.12 Torque-To-Balance Drift Stability

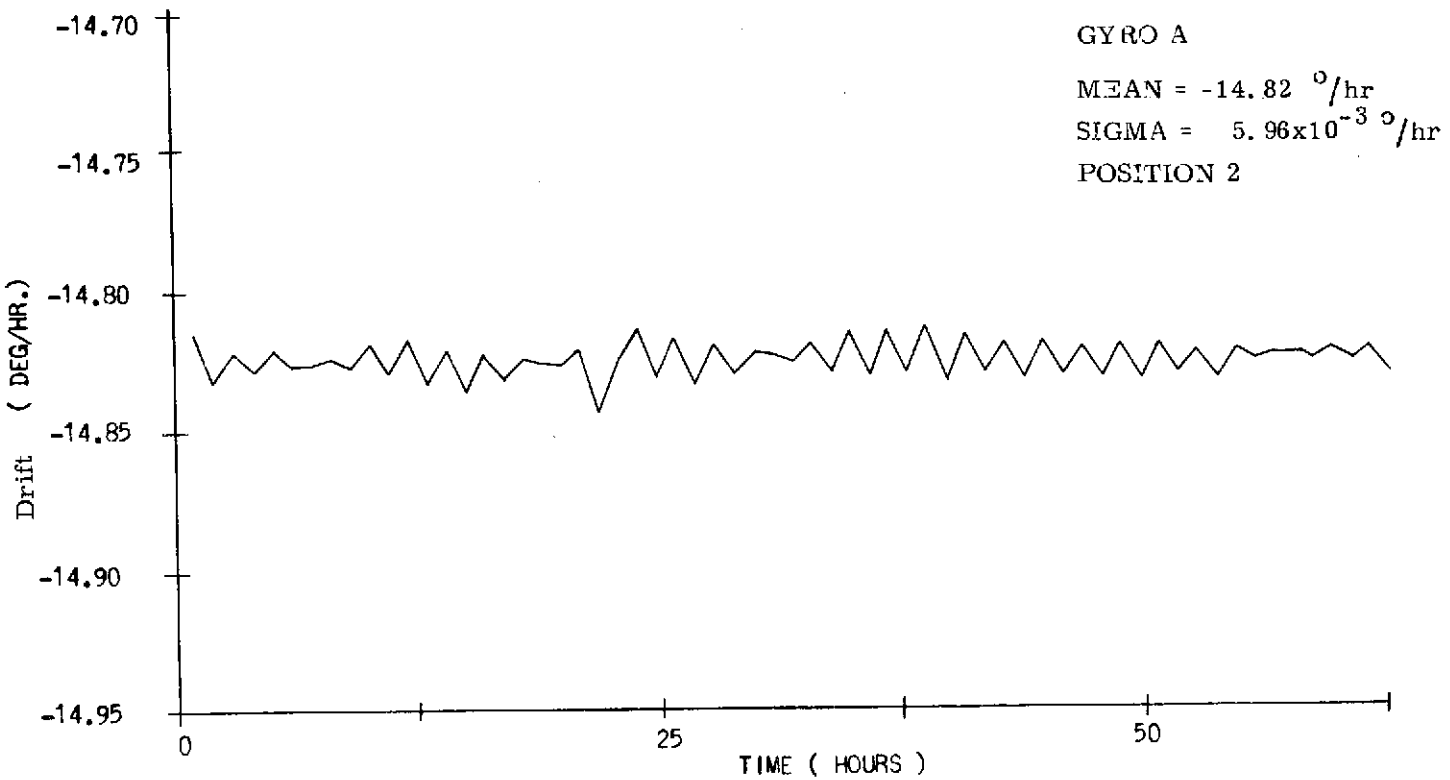

Fig. 4.13 Fixed Position Gyro Drift Stability

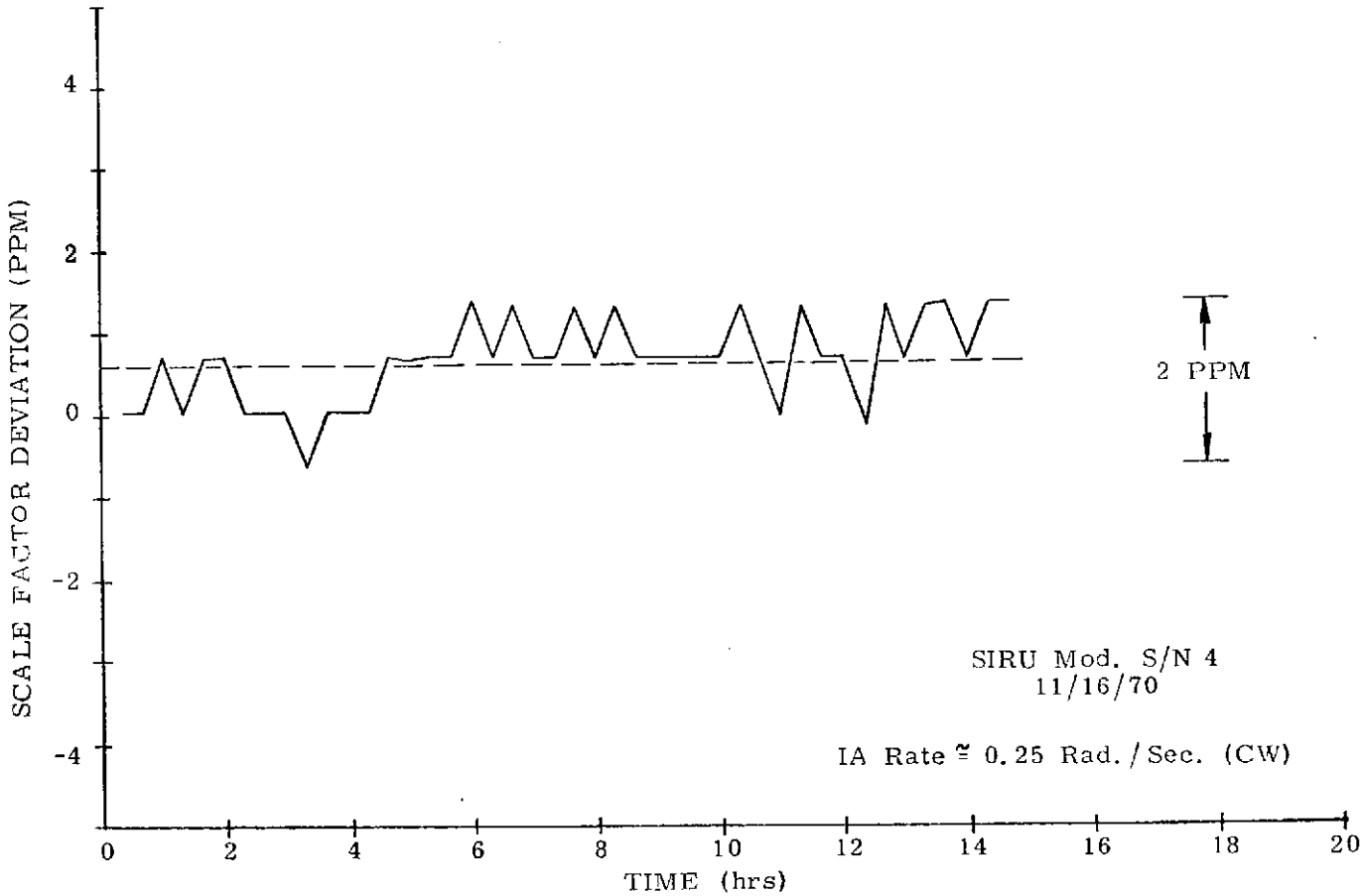

Fig. 4.14 Scale Factor Stability Data

5.0 Gyro Test

Gyro testing is performed with the instrument either in or out of the gyro module using the equipment and test techniques described below.

5.1 Test Equipment

A SIRU gyro module under component level test is shown in Fig. 5.1. The clock, dc axis supply and module break-outs are mounted on the table top. The table can be controlled in an inertial reference mode, locked at fixed positions or driven at constant rates.

A PDP 8/L computer Fig. 5.2 performs on-line computation and display for the various test modes. To measure SF vs input rate, the computer sequences the table through a series of rates through a D/A converter, Fig. 5.3. The operator can input test options and instrument data through the teletype. As outputs, the computer prints out table rate, table direction, and SF deviation from nominal. The computer is also used to perform on-line SF stability or drift coefficient measurements.

5.2 Test Techniques

Gyro tests can be divided into three general classifications:

1. Instrument Acceptance Tests
2. SIRU Module Calibration Tests
3. Interpolator Retrofit Tests

Each of these types of test are described briefly in the following paragraphs.

Instrument Acceptance Tests

These tests, performed at the gyro manufacturer's test laboratory, determine the integrity of gyro construction. The tests include a float freedom test to check for contaminated or mechanical restrictions, drift stability after exposure to room temperature cooldowns to insure structural integrity, PMT magnetization and operational tests, and the measurement of gyro motor starting characteristics.

Fig. 5.1 Gyro Module Component Testing

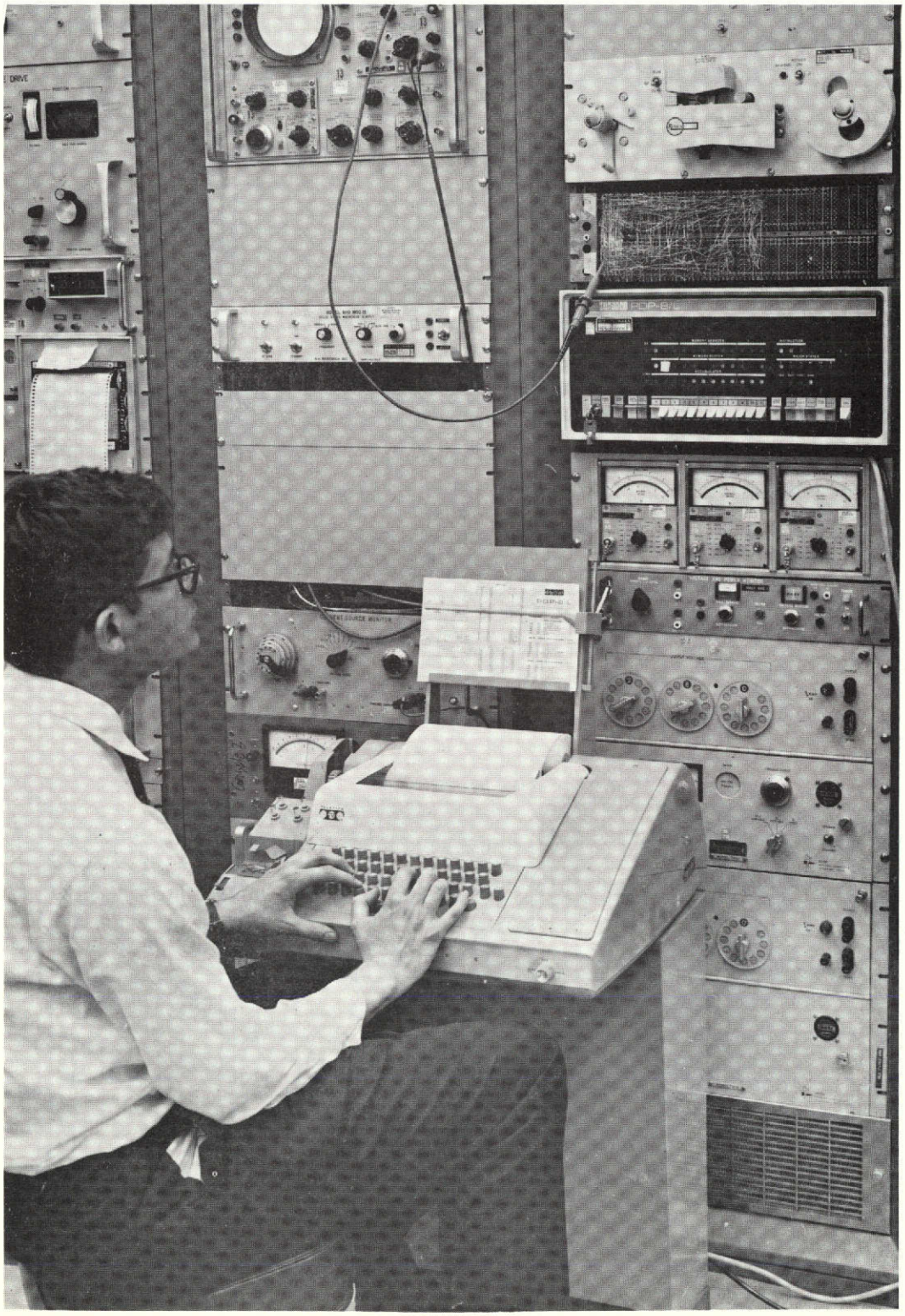

Fig. 5.2 Testing Computation and Display Facilities

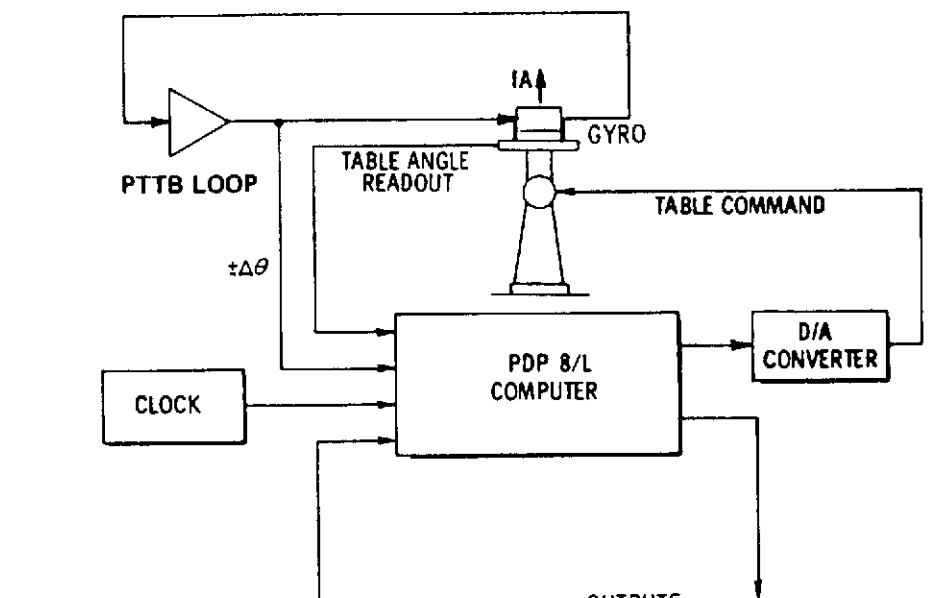

INPUTS

1. NUMBER REVS PER SF COMPUTATION
2. NUMBER OF TIMES TO REPEAT SF COMPUTATION AT EACH TABLE RATE
3. EARTH RATE GYRO DRIFT CORRECTION
4. NOMINAL GYRO SCALE FACTOR

OUTPUTS

1. TABLE RATE
2. SF DEVIATION FROM NOMINAL
3. MAX AND MIN VALUE OF SF AT EACH RATE
4. PUNCHED PAPER TAPE FOR PLOT

Fig. 5.3 On-Line Scale Factor Determination

SIRU Module Calibration Tests

These tests include checking out the instrument and submodules, selection of trim components, aligning the input axis and normalization of the module. Calibration data such as SF magnitude and variation with input rate, drift coefficients and input axis alignments are obtained on the covered module for system module integration.

The torquer SF is adjusted to 44.0629 $\widehat{\text{sec}}$/pulse with a tolerance of 0 to 200 ppm.

The input axes are aligned to within 10 $\widehat{\text{sec}}$ about the OA and SRA.

Due to the uniquenessof the SIRU angle and the alignment accuracies required, the alignment procedure is described in more detail below.

The alignment is accomplished by mounting a precision alignment fixture on the table such that the alignment pins on surface A and B are accurately located with respect to the table rotary axis within two $\widehat{\text{sec}}$. (See Fig. 5.4).

The gyro is mounted on surface A and driven at a constant table rate. The alignment of the IA about the OA is accomplished for this orientation by adjusting the alignment screws. The gyro is then mounted on surface B. The table is driven at a constant rate to determine and adjust the IA alignment about the SRA axis.

Interpolator Retrofit Tests

Most modules were initially assembled and delivered to the system without an Interpolator/Compensator. The modules were later recycled for an interpolator retrofit. After this retrofit calibration tests were rerun.

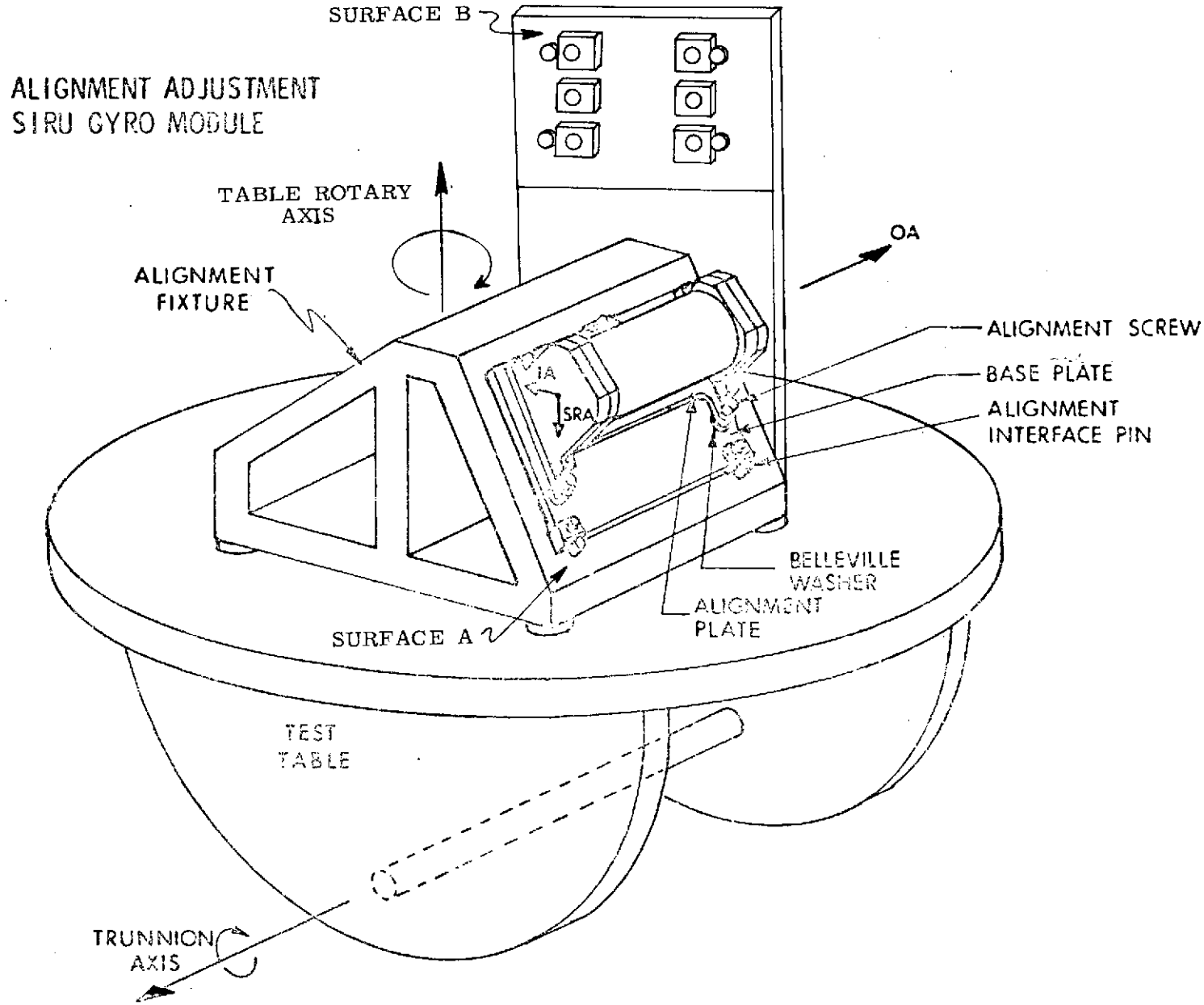

Fig. 5.4 Alignment Adjustment SIRU Gyro Module

APPENDIX A
GYRO MODULE PARAMETERS

1.0 Introduction

The principle parameters of the gyro module as implemented for the SIRU system are summarized in this appendix. They represent performance consistent with the goals contained in the original NASA Statement of Work and subsequent cost effective design tradeoffs.

2.0 Scale Factor Nominal Parameters

$\Delta\theta$ Pulse	$2^{-13} + 2^{-14} + 2^{-15}$ radians = 44.1 $\widehat{sec}$
SF Decay Characteristics	Nominal 40 ppm/decade, maximum 60 ppm/decade
Interrogation Rate (Max Pulse Rate)	4800 pps ± 1/2 ppm = F_1
Loop Torque Rate Capability	1.025 rad/sec (1.0 minimum)
Torquer Duty Cycle	(15/16) ($1/F_1$) = 195 microseconds of 208 microseconds
Stability	0.25 rad/sec in 24 hours (15 ppm p-p)
Stabilization Time	One hour
SF Linearity	± 30 ppm p-p
SF Thermal Sensitivity	1/2 ppm/^{o}F
SF Voltage Sensitivities	
PVR Supply	1 ppm/.05%
40v Supply	1 ppm/1% (within ±5% range)
SF Dynamic Sensitivity	
Radial Displacement	25 ppm/rad/sec about OA
Axial or Radial g Loading	5 ppm/g

3.0 IA Alignment

Thirty day stability with 3 room temperature cooldowns	5 $\widehat{sec}$ (rss)
Alignment Repeatability (removal and replacement)	10 $\widehat{sec}$ (rss)

4.0 Operational Characteristics

4.1 Power Supply Characteristics

a. DC

	Source Level	Load (Max)	Ripple
1.	40.0 vdc ± 0.4 vdc	165 ma	<0.43 v_{rms}
2.	15.000 vdc ± 0.008 vdc	11 ma	<0.002 v_{rms}
3.	-10.0 vdc ± 0.5 vdc	25 ma	<0.140 v_{rms}
4.	10.0 vdc ± 0.5 vdc	25 ma	<0.140 v_{rms}
5.	5.25 vdc ± 0.25 vdc	140 ma	<0.1 v_{rms}
6.	28 vdc ± 3 vdc	750 ma	<0.5 v_{rms}
7.	28 vdc ± 0.5 vdc	55 ma	<0.3 v_{rms}
8.	-20 vdc ± 1.0 vdc	25 ma	<0.2 v_{rms}

b. AC

1. 9600 Hz, 8.0 v_{rms} ± 1%, 2.5 watts max, harmonic content < 2% sinewave
2. 800 Hz, 2 phase, 28 v_{rms} ± 5%, 2.6 watts max each phase, phase A leads phase B by 90^{o} ± 0.5^{o}, harmonic content < 20%
3. 9600 Hz and 800 Hz signals in synchronization

4.2 Timing Pulse Characteristics

Interrogate pulse	
Amplitude	4.5 ± 0.5 vdc
Width	0.4 microseconds
Repetition Rate	4.8 kpps
Switch pulse pair	
Amplitude	4.5 ± 0.5 vdc
Width	0.4 microseconds
Spacing	13 microseconds
Repetition Rate	4.8 kpps
Lag of reset pulse to interrogate pulse	2 microseconds ± 1/2 microseconds

4.3 Output Signal Requirements

$\Delta\theta$ pulses	2 microseconds width, +5 vdc amplitude
Interpolator pulses	4.5 ± 0.5 vdc amplitude, 0 to 31 pulses at 1.5 mc rate, 200 nanoseconds width, first pulse starts 10 microseconds ± 1 microsecond after interrogate pulse leading edge
Interpolator end-of-data pulse	4.5 ± 0.5 vdc amplitude, 200 nanoseconds width, 208.33 microseconds repetition rate, pulse occurs 31.34 microseconds after interrogate pulse leading edge.

4.4 Monitoring Line Identification

1. PVR power test point
2. Single ended SG monitor point, 1250 mv/milliradian of angular input about IA at 9600 Hz
3. SF resistance test point
4. Gyro temperature sensor #4, 500 ohms ± 0.5 ohms at operating temperature (+.00226 ohms/ohm/^{o}F).
5. DC amplifier test point

4.5 Auxiliary Input Requirements

1. 0 to 28 vdc at 0 to 0.4 amp (for adjustable fixed heat when used with GSE only).
2. Frequency and Timing Accuracy and Stability— All ac input voltage frequencies and input signal repetition rates are derived from a clock whose basic frequency is 3.6864000 mega Hz ± 1 part in 10^{8} with a stability of ±3 parts in 10^{7} per week.

4.6 Thermal Characteristics

Nominal Thermal Dissipation	21.5 watts
Thermal Dissipation Limits	17 watts to 30 watts
Nominal Average Module Mounting Pad Temperature	105^{o}F Max p-p deviation between pads and average temperature ±3^{o}F

Temperature Control Range (at 70°F nominal, free air ambient & 1/2 inch insulation) 60° to 110°F

5.0 Gyro Module Connector—Pin Identification

Pin Identification—SIRU Gyro Module Connector

Pin #	Line Designation
1.	$+\Delta\theta$ Hi
2.	$+\Delta\theta$ Lo
3.	Interrogate Pulse Hi
4.	Interrogate Pulse Lo
5.	GSE Sensor Hi
6.	GSE Sensor Lo
7.	-20 vdc
8.	-20 vdc return
9.	Gyro Temp. Sensor #4 Hi
10.	Scale Factor TP Hi
11.	DC Amp TP Hi
12.	Interpolator end of data Hi
13.	Structure Ground
14.	9600 Hz Hi
15.	+40.0 vdc
16.	+40.0 vdc Ret
17.	+15 vdc PVR Shield
18.	+15 vdc PVR
19.	$+\Delta\theta$ shield
20.	$-\Delta\theta$ shield
21.	Interrogate Pulse Shield
22.	Switch Pulse Shield
23.	GSE HTRS Lo
24.	Interpolator Data Pulse Lo
25.	Interpolator Data Pulse Shield
26.	Gyro Temp Sensor #4 Lo
27.	PVR TP Hi
28.	PVR TP Return
29.	Signal Generator TP Lo
30.	Interpolator End of Data Lo
31.	800 Hz Lo

32.	9600 Hz Lo
33.	-10 vdc
34.	+5 vdc
35.	+15 vdc PVR Return
36.	$-\Delta\theta$ Hi
37.	$-\Delta\theta$ Lo
38.	Switch Pulse Hi
39.	Switch Pulse Lo
40.	GSE Heaters Hi
41.	Interpolator Data Pulse Hi
42.	+28 vdc Unregulated
43.	+28 vdc Unregulated Return
44.	+28 vdc Regulated
45.	Signal Generator TP Shield
46.	Signal Generator TP Hi
47.	Interpolator End of Data Shield
48.	800 Hz ϕB
49.	800 Hz ϕA
50.	0 vdc (+10 vdc; -10 vdc; +5 vdc Return)
51.	+10 vdc